TECHNICAL INFORMATION SERIES

R63SD40

THEORY OF HYPERSONIC LAMINAR STAGNATION REGION HEAT TRANSFER IN DISSOCIATING GASES

S.M. SCALA
L.M. GILBERT

SPACE SCIENCES LABORATORY
GENERAL ELECTRIC
MISSILE AND SPACE DIVISION

SPACE SCIENCES LABORATORY

AEROPHYSICS SECTION

THEORY OF HYPERSONIC LAMINAR STAGNATION REGION HEAT TRANSFER IN DISSOCIATING GASES

by

S. M. Scala
L. M. Gilbert

Work performed under NASA Contract
Number NAS 7-100

R63SD40
April, 1963

MISSILE AND SPACE DIVISION

GENERAL ELECTRIC

CONTENTS

LIST OF FIGURES

ABSTRACT

Several earlier investigators who have considered hypersonic gas dynamic heating have suggested the use of empirical correlation formulas such as:

$$Q_w \sqrt{R_B} = C \sqrt{\rho_\infty} \quad V_\infty^3$$

where Q_w is the stagnation point heat transfer rate, R_B is the vehicle nose radius, ρ_∞ is the ambient density and V_∞ is the flight speed of the vehicle.

However, since the magnitude of the coefficient C depends on the contribution of the actual chemical species present in a given planetary atmosphere, C is not known "a priori" but can be obtained theoretically by solving the multicomponent boundary layer equations for a variety of foreign gases, which has not been accomplished heretofore.

The purpose of the present investigation, therefore, was to determine the thermochemical effects of foreign planetary atmospheres upon hypersonic stagnation region laminar heat transfer and skin friction, and to attempt to obtain, if possible, a simple correlation of the results with molecular weight, over a range of free stream molecular weight from 2 to 44.

SYMBOLS

A	Angstroms
B_i	referred mole fraction of species i
C_i	mass fraction of species i
C_{p_i}	specific heat of the i^{th} species at constant pressure
$\overline{C}_p$	frozen specific heat of mixture
$\mathscr{D}_{ij}$	binary diffusion coefficient
D_{ij}	multicomponent diffusion coefficient
f	dimensionless stream function, distribution function
$\underrightarrow{F}$	external force
h_i	static enthalpy of the i^{th} species, including chemical
h	static enthalpy of the mixture
$\Delta h^o_{f_i}$	enthalpy of formation of the i^{th} species
k	Boltzmann's constant
K	frozen thermal conductivity of the mixture
K_p	equilibrium constant
$\mathcal{M}_i$	molecular weight of species i
M_i	mass of species i

$\overline{\mathcal{M}}$	mean molecular weight of the gas mixture
$\dot{m}_i$	mass flux of species i
P	static gas pressure, momentum
Q	heat transfer, collision cross section
$\mathcal{R}$	universal gas constant
R_B	body radius
t	time
T	temperature
u, v	velocity components
$\underset{\rightarrow}{v}$	macroscopic gas velocity
$\underset{\rightarrow}{v}_i$	absolute velocity of species i
$\underset{\rightarrow}{V}_i$	diffusion velocity of species i
V_∞	flight speed
$\dot{w}_i$	chemical source term, net mass rate of production of species i per unit volume by chemical reaction
X_i	mole fraction of species i
x, y, r	coordinate system
β	pressure gradient parameter
γ	ratio of specific heats
η, ξ	similarity variables

$\theta = \frac{T}{T_e}$	dimensionless temperature
μ_i	viscosity of the i^{th} species
$\underset{\sim}{\pi}$	pressure tensor
ρ	density
σ	collision diameter
τ	shear stress
$\varphi = \frac{X}{R_B}$	body coordinate angle
Ω^*	collision integral

Subscripts

e	edge of viscous layer
g	gas
i	i^{th} species
Min.	minimum
Mix.	mixture
s	stagnation region
w	wall, surface of vehicle
∞	upstream, ambient conditions
2	downstream, behind normal shock
η	denotes differentiation with respect to η

Dimensionless Groups

$$C_H = \frac{Q_w}{\rho_\infty V_\infty (H_e - h_w)}$$, Stanton number

$$C_f = \frac{\tau_w}{1/2\ \rho_\infty V_\infty^2}$$, skin friction coefficient

$$\ell = \frac{\rho\mu}{\rho_w\ \mu_w}$$

$$L_{ij} = \frac{\rho \overline{C}_p D_{ij}}{K}$$, multicomponent Lewis number

$$Nu = \frac{Q_w \overline{C}_{p_w} x}{K_w (H_e - h_w)}$$, Nusselt number

$$Pr = \frac{\mu \overline{C}_p}{K}$$, Prandtl number

$$Re_s = \frac{\rho_\infty V_\infty R_B}{\mu_e}$$, shock Reynolds' number

$$Re_w = \frac{\rho_w U_e x}{\mu_w}$$, wall Reynolds' number

INTRODUCTION

With the advent of space exploration, interest is growing in the problem of entry into planetary atmospheres other than Earth. Thus, the problem of predicting the aerodynamic heat transfer rate becomes complicated by the presence of chemical species other than those present in high temperature air.

The theoretical investigations of the determination of heating rates in dissociating air flows are well documented and some representative studies concerning this problem area appear in References 1 to 5. A comparison (Ref. 5) between these various theoretical predictions of stagnation point heating in dissociated air indicates good agreement with a maximum deviation of approximately $\pm$ 20 per cent from a mean value.

The problem of predicting the stagnation point heat transfer in gases other than air has led some of the earlier (Ref. 6 - 10) investigators to suggest the use of generalized correlation formulas such as:

$$Q_w \sqrt{R_B} = C \sqrt{\rho_\infty} V_\infty^3 \tag{1}$$

In the above equation, the value of the coefficient C is intended to reflect the contributions of the various chemical species present in any atmosphere to the transport and thermodynamic properties of the resulting dissociated gas mixture.

Gazley (Ref. 6) estimates the coefficient C to be proportional to the square root of the ratio of the free stream Mach number to the Reynolds' number for the laminar continuum regime of planetary entry. This calculation leads to values for C

which are similar for Earth, Mars and Venus to within $\pm$ 3 per cent. Chapman (Ref. 7) relies on the dissociated air theory of Lees (Ref. 2) to obtain estimates of heating rates in gases other than air and finds that $C \sim Pr^{1/2} \mu_o^{1/2} (\gamma - 1/\gamma)^{1/4}$. In another study, Lees (Ref. 8) offers an equation for engineering purposes in which the constant C is to be taken the same for the planets Earth, Mars and Venus. In his correlation equation, however, provision is made for the variation of surface temperature.

The first rigorous theoretical investigation of hypersonic heat transfer in a gas different from air was that performed by Hoshizaki (Ref. 10). In his study, Hoshizaki calculates the equilibrium boundary layer flow at the stagnation point of a blunt body in carbon dioxide gas as well as in air. Preferential diffusion of the various chemical species is neglected, and the effects of dissociation are taken into account by means of the "total" thermodynamic and transport property concept, (Ref. 11, 12, 13). Hoshizaki's correlated heating rates in air compare favorably with the earlier theoretical studies of Lees (Ref. 8) and Chapman (Ref. 7). Furthermore, he finds that the coefficient C for CO_2 is **approximately 10 per cent higher than that for air.**

Experimental efforts to determine heat transfer in gases other than air include hypersonic shock tube (Ref. 14, 15) and ballistic range (Ref. 16) measurements in pure nitrogen, pure carbon dioxide and mixtures of nitrogen, carbon dioxide and argon.

The intent of this present study is to consider the thermochemical effects rigorously and to determine theoretically the aerodynamic heat transfer rate and skin

friction at the surface of a vehicle traveling at hypersonic speed in a planetary atmosphere of arbitrary chemical composition. In order to accomplish this end, the laminar heating rates and surface shear stresses in eight dissociating gas mixtures having various degrees of chemical complexity are first determined. Then, simple correlation equations based on the molecular weights of the undissociated gases are derived.

The gaseous systems considered in this study are as follows: three diatomic gases including H_2, N_2, and O_2; a triatomic gas, CO_2; and several mixtures including four component "Air", i.e., O, O_2, N and N_2 (simulating Earth's atmosphere), and several six component mixtures of the dissociation products of N_2 and CO_2, i.e., CO_2, CO, O_2, O, N_2 and N (simulating the Martian and Venusian atmospheres).

The approach used in this study consists of first selecting a suitable gas model based on the predominant species existing in the particular planetary atmosphere under investigation. The next step is the determination of the thermochemical properties of the gas existing in the flow field between the detached shock wave and the entry vehicle, by solving the normal shock and isentropic stagnation relations assuming thermochemical equilibrium. Finally, the theoretical laminar heat transfer rates are determined from the exact solutions of the multicomponent laminar boundary layer equations, as is the skin friction coefficient.

In this study it is necessary to solve the normal shock equations and isentropic stagnation equations in order to provide self-consistent outer boundary conditions for the boundary layer computations. Also, by this means, it is possible to relate unequivocally the boundary layer solutions to the external ambient conditions for each of the gas systems under consideration.

The appropriate governing boundary layer equations for a compressible viscous multicomponent chemically reacting gas are presented, and the transport and thermodynamic properties of the gaseous mixture are evaluated as a function of the equilibrium gas composition and temperature. In the numerical integration of the boundary layer equations, the Prandtl number of the mixture and the multicomponent Lewis numbers are evaluated at the surface conditions. The viscosity of the mixture and all thermodynamic coefficients are evaluated locally throughout the viscous layer. The surface and outer edge boundary conditons are satisfied, assuming that the gas is in a state of local thermochemical equilibrium throughout the boundary layer. Numerical solutions are obtained on an IBM 7090 digital computer, and the results presented in the form of correlation equations and graphs. The calculations cover an appropriate range of flight speeds (i.e., approximately 10,000 to 50,000 ft./sec.) necessary to correlate the dissociation effects for each of the gaseous systems considered.

In addition to the correlated heat transfer rate, the skin friction coefficients are also correlated, and are presented for the gaseous systems treated. Comparisons are made between the shear stress and heat transfer, and the agreement with Reynolds' analogy is noted. Finally, the new theoretical results are compared with other available theoretical predictions and available experimental data. The agreement with other theoretical results and with experimental data is found to be good.

THERMOCHEMISTRY

Let us first consider the determination of the thermochemical state of the gas surrounding a space vehicle during planetary entry. During hypersonic flight, in a planetary atmosphere, the free stream gas is dissociated and perhaps partially ionized by the shock wave which precedes the vehicle. For known ambient conditions in the free stream gas (i.e. pressure, temperature, density and chemical composition) and for a given flight speed, one is able to determine the downstream conditions behind the shock wave by a simultaneous solution of the Rankine-Hugoniot relations together with an appropriate equation of state.

These algebraic equations may be written:

$$\rho_\infty V_\infty = \rho_2 V_2 \tag{2}$$

$$P_\infty + \rho_\infty V_\infty^2 = P_2 + \rho_2 V_2^2 \tag{3}$$

$$h_\infty + \frac{V_\infty^2}{2} = h_2 + \frac{V_2^2}{2} \tag{4}$$

and represent the conservation of mass, momentum and energy across a normal shock wave, respectively. Equations 2, 3, and 4 relate the density, the gas velocity, the pressure and the enthalpy at the upstream location ∞ to the downstream location 2 behind the shock. In addition to the above conservation equations, one must introduce an appropriate equation of state for the gas mixture in order to solve this system of equations.

$$P = \rho \frac{\mathcal{R}}{\mathcal{M}} T \tag{5}$$

The chief difficulty in solving this set of equations resides in the fact that in a chemically reacting gas, the enthalpy and the mean molecular weight are functions of the gas composition. The composition of this gas is in turn a function of the unknown

temperature and pressure, and hence an iterative solution is required. Therefore, in order to proceed, one requires a knowledge of the equilibria of the resulting high temperature gaseous system downstream of the shock wave.

In general, the coupling of the high temperature equilibrium thermodynamic properties of the gaseous system under study to the normal shock equations may be done in two ways. The most popular numerical procedure (for normal shock waves in air, Ref. 17-20) has been to store tabular data in the form of Mollier charts for the ranges of temperature, pressure, density, enthalpy, etc. likely to be encountered. The alternate procedure is to compute the necessary thermodynamic properties of the dissociated gas mixture as part of the numerical solution of the overall problem, (Ref. 21 and 22).

The second of these methods is the procedure which was used in this study. This method, while being somewhat restrictive in terms of the number of chemical species one may conveniently handle numerically, is extremely flexible in that the relative abundance of any given chemical element in a particular system may be varied parametrically by simply changing one or more constants.

Consider a planetary atmosphere in which the ambient undisturbed gas ahead of the shock wave is characterized, for example, by a mixture of carbon dioxide, molecular nitrogen and argon. The number and type of chemical species present in the flow field between the shock wave and the entering space vehicle will, of course, depend upon the shock strength. For flight velocities sufficiently high to cause dissociation of the gas, one may expect the following chemical species to be present: CO_2, CO, C, C_2, O, O_2, N, N_2, A, NO, CN, etc. While it is not practical, nor indeed necessary, to consider all of the possible chemical species (since some appear in only trace amounts), one can discuss, in general, an n component system and the n independent relationships necessary for the solution of the mathematical system.

In order to determine the composition of an n component chemically reacting gas mixture originating from k chemical elements, one has available k-1 relationships for the conservation of chemical elements, one relationship for the overall conservation of species, and n-k relationships dealing with the rate at which the chemical reactions are progressing. We begin with relationships for the conservation of chemical elements, which, for our purposes, take the form of mass balance ratios.

For this system composed of four chemical elements (i.e. oxygen, nitrogen, carbon and argon) one may write three mass balance ratios as follows:

$$\frac{\tilde{C}}{\tilde{N}} = k_1 \; ; \; \frac{\tilde{O}}{\tilde{N}} = k_2 \; ; \; \frac{\tilde{A}}{\tilde{N}} = k_3 \tag{6}$$

In this notation, the mass of the chemical element (oxygen for example) is defined in terms of the mass fractions in the following manner.

$$\tilde{O} = C_O + C_{O_2} + \mathcal{M}_O \sum_i \left(\frac{C_i}{\mathcal{M}_i} \right)_O + \mathcal{M}_{O_2} \sum_{j \neq i} \left(\frac{C_j}{\mathcal{M}_j} \right)_{O_2} \tag{7}$$

In equation 7 the first two mass fractions account for the atomic and molecular oxygen in the free state. The first summation quantity includes all the atomic oxygen in a chemically bound (i.e. CO, NO) state, and the second summation quantity includes all of the chemically bound molecular oxygen. The masses of the other chemical elements are defined in a similar manner.

The values of the three constants k_1, k_2, and k_3 are given by the relative abundance of the chemical species in the undissociated ambient atmosphere. As an example, k_2 is evaluated below.

$$k_2 = \frac{\tilde{O}}{\tilde{N}} = \frac{\left(\mathcal{M}_{O_2} / \mathcal{M}_{CO_2} \right) C_{CO_{2\infty}}}{C_{N_{2\infty}}} \tag{8}$$

The relationship for the overall conservation of species takes the form of Dalton's Law for a static system in thermochemical equilibrium, and provides us

with the condition that the sum of all the mole fractions must be unity.

$$\sum_i X_i = 1.0 \tag{9}$$

where i is the i^{th} chemical species in the n component mixture.

For the case where the gas has equilibrated itself both thermally and chemically, the remaining n-k relationships are available in the form of the equilibrium functions. The assumption of thermochemical equilibrium implies that the characteristic chemical reaction times are several orders of magnitude smaller than the available flow times and that the dissociation and recombination rates of the various chemical reactions are effectively infinitely fast. An example is shown below which considers the chemical reaction involving carbon monoxide, atomic oxygen and atomic gaseous carbon.

$$C(g) + O \rightleftharpoons CO$$

$$K_{p_{CO}} = \frac{X_{CO}}{X_{C(g)} X_O P} \tag{10}$$

In the above, P is the pressure of the gas mixture, expressed in atmospheres. The K_P functions themselves are exponentially dependent upon the temperature, and for large ranges in temperature may be expressed in a simple Arrhenius form. The auxiliary relationships for the system are the expressions for the mass fractions and mean molecular weight:

$$C_i = \frac{X_i \mathcal{M}_i}{\overline{\mathcal{M}}} \; ; \; \overline{\mathcal{M}} = \sum_i X_i \mathcal{M}_i \tag{11}$$

After the composition of the gas has been determined at a given pressure and temperature, the enthalpy of the gas mixture may be calculated by means of the relationship:

$$h = \sum_i C_i h_i \tag{12}$$

The enthalpy of a pure species, h_i, is given as:

$$h_i = \int_{T_{ref.}}^{T} C_{p_i}\, dT + \Delta h_{f_i}^{o} \tag{13}$$

where $\Delta h_{f_i}^{\circ}$ is the enthalpy of formation at the reference temperature.

It is noted that the resulting system of n algebraic equations is highly coupled and extremely non-linear and, in general, for $n > 2$, iterative techniques must be employed in order to obtain a solution to the system.

We will now apply these general equations to the specific gas systems under consideration. The pure diatomic gas systems (i.e. oxygen, nitrogen, and hydrogen) each contain a single chemical element and hence the mass balance ratios (equations 6) are not required. Furthermore, the atomic and molecular species in equilibrium are directly determined by utilizing their K_P relationship. Therefore, the composition of each diatomic gas system is determined by equation 9 together with the appropriate K_P function. The equilibrium reactions for the various diatomic systems are as follows:

Diatomic oxygen system:

$$O_2 \rightleftharpoons 2O$$

$$K_{P_O} = \frac{X_O^2\, P}{X_{O_2}} \tag{14}$$

Diatomic nitrogen system:

$$N_2 \rightleftharpoons 2N$$

$$K_{P_N} = \frac{X_N^2\, P}{X_{N_2}} \tag{15}$$

Diatomic hydrogen system:

$$H_2 \rightleftharpoons 2H$$

$$K_{P_H} = \frac{X_H^2\, P}{X_{H_2}} \tag{16}$$

The triatomic gas (CO_2) considered here contains two chemical elements and requires a singe mass balance ratio as follows:

$$k_1 = \frac{\tilde{O}}{\tilde{C}} = \frac{\left(m_{O_2}/m_{CO_2}\right) C_{CO_2}}{\left(m_C/m_{CO_2}\right) C_{CO_2}} = \frac{32}{12} \tag{17}$$

In the dissociated mixture, we will consider a model consisting of the five species, CO_2, CO, O_2, O and C (g). Therefore, in addition to equations 9 and 17, three equilibrium relationships are needed to complete the system. Two of these are given by equations 10 and 14 and the third is shown below:

$$CO + O \rightleftharpoons CO_2$$

$$K_{P_{CO_2}} = \frac{X_{CO_2}}{X_{CO}\, X_O\, P} \tag{18}$$

In the analysis of heat transfer phenomena, high temperature dissociated air is closely approximated by a four component mixture of atomic and molecular oxygen and nitrogen. The single mass balance ratio required for this system is:

$$k_2 = \frac{\tilde{O}}{\tilde{N}} = \frac{C_O + C_{O_2}}{C_N + C_{N_2}} = 0.3068 \tag{19}$$

Equation 19 states that the composition of equilibrium air is 23.48 % oxygen and 76.52% nitrogen by mass in the free stream. Dalton's Law (equation 9), is, of course, used for all the gas systems. The two remaining equilibrium functions for the "Air" system are given by equations 14 and 15.

Six chemical species are treated in the system for the C-O-N gaseous mixture, including CO_2, CO, O_2, O, N_2 and N. Of the two mass balance ratios required for this system, one is given by equation 17 and the other is shown below.

$$k_2 = \frac{C_O + C_{O_2} + \left(m_O/m_{CO}\right) C_{CO} + \left(m_{O_2}/m_{CO_2}\right) C_{CO_2}}{C_N + C_{N_2}} \tag{20}$$

In the C-O-N system, the numerical value of k_2 was altered to simulate three mixtures, corresponding to 90% CO_2 - 10% N_2, 50% CO_2 - 50% N_2 and 10% CO_2 - 90% N_2. The equilibrium relationships for this system are given by equations 14, 15 and 18.

Having chosen a particular system for study together with a set of ambient free-stream conditions, the state of the gas is first determined at point 2 behind the normal shock by solution of equations 2 through 5. Then, an isentropic calculation (see reference 22) is performed along the stagnation stream line. A compatible set of boundary conditions at the outer edge of the boundary layer is thus determined.

BOUNDARY LAYER CONSIDERATIONS

The non-linear partial differential equations of change for a multicomponent chemically reacting gas are derived, for example, in Ref. 23 and include the conservation of mass, chemical species, momentum and energy as shown below:

$$\frac{\partial \rho}{\partial t} + \nabla \cdot (\rho \underset{\rightarrow}{v}) = O \tag{21}$$

$$\frac{\partial \rho_i}{\partial t} + \nabla \cdot (\rho_i \underset{\rightarrow}{v}_i) = \dot{w}_i \tag{22}$$

$$\rho \frac{d \underset{\rightarrow}{v}}{dt} = \nabla \cdot \underset{\sim}{\pi} + \sum_i \rho_i \underset{\rightarrow}{F}_i \tag{23}$$

$$\rho \frac{de}{dt} = - \nabla \cdot \underset{\rightarrow}{Q} + \underset{\sim}{\pi} : \nabla \underset{\rightarrow}{v} + \sum_i \rho_i \underset{\rightarrow}{V}_i \cdot \underset{\rightarrow}{F}_i \tag{24}$$

Upon introducing the boundary layer approximation for a body-oriented coordinate system (see Figure 1), the conservation of mass becomes (Ref. 24):

$$\frac{\partial}{\partial x} \left(\rho r^{\delta} u \right) + \frac{\partial}{\partial y} \left(\rho r^{\delta} v \right) = O \tag{25}$$

In the absence of thermal diffusion, the conservation equation for species i becomes:

$$\rho \mathcal{M}_i \left(u \frac{\partial B_i}{\partial x} + v \frac{\partial B_i}{\partial y} \right) + \frac{\partial}{\partial y} \left[\sum_{j \neq i} \frac{\mathcal{M}_i \mathcal{M}_j}{\bar{\mathcal{M}}^2} \rho D_{ij} \frac{\partial X_j}{\partial y} \right] = \dot{W}_i \qquad (26)$$

where $B_i = X_i / \bar{\mathcal{M}}$

The stream wise component of momentum becomes:

$$\rho u \frac{\partial u}{\partial x} + \rho v \frac{\partial u}{\partial y} = - \frac{\partial P}{\partial x} + \frac{\partial}{\partial y} \left(\mu \frac{\partial u}{\partial y} \right) \qquad (27)$$

The normal component of momentum is:

$$\frac{\partial P}{\partial y} = 0 \qquad (28)$$

The energy equation becomes:

$$\rho \bar{C}_p \left(u \frac{\partial T}{\partial x} + v \frac{\partial T}{\partial y} \right) = u \frac{\partial P}{\partial x} + \mu \left(\frac{\partial u}{\partial y} \right)^2 + \frac{\partial}{\partial y} \left(K \frac{\partial T}{\partial y} \right) - \sum_i C_{p_i} \frac{\partial T}{\partial y} \sum_{j \neq i} \frac{\mathcal{M}_i \mathcal{M}_j}{\bar{\mathcal{M}}^2} \rho D_{ij} \frac{\partial X_j}{\partial y} - \sum_i \dot{w}_i h_i \qquad (29)$$

Upon introducing the Mangler-Dorodnitsyn (Ref. 2) transformations

$$\eta = \frac{\rho_e u_e}{\sqrt{2\xi}} \int_o^y r^\delta \frac{\rho}{\rho_e} dy \qquad (30)$$

$$\xi = \int_o^x \rho_w \mu_w u_e r^{2\delta} dx \qquad (31)$$

and assuming that local similarity holds, then equations 25 through 29 may be reduced to a set of ordinary non-linear differential equations. The diffusion equation for the i^{th} chemical species becomes:

$$\left[\frac{\ell}{Pr} \sum_{j \neq i} \frac{\mathcal{M}_i \mathcal{M}_j}{\bar{\mathcal{M}}^2} L_{ij} X_{j_\eta} \right]_\eta - f \mathcal{M}_i B_{i_\eta} = \frac{\beta}{\left(\frac{du_e}{dx} \right)} \frac{\dot{w}_i}{\rho} \qquad (32)$$

where $\beta = 2\, d\ln u_e / d\ln \xi$ and the stagnation point velocity gradient is assumed to be Newtonian.

The conservation of momentum becomes:

$$\left(\ell f_{\eta\eta} \right)_\eta + f f_{\eta\eta} + \beta \left[\frac{\rho_e}{\rho} - f_\eta^2 \right] = 0 \qquad (33)$$

The energy equation becomes:

$$\left(\frac{\bar{C}_p \ell \theta_\eta}{P_r}\right)_\eta + \bar{C}_p f \theta_\eta - \sum_i \frac{C_{p_i} \ell}{Pr} \theta_\eta \sum_{j \neq i} \frac{\mathcal{M}_i \mathcal{M}_j}{\bar{\mathcal{M}}^2} L_{ij} X_{j_\eta}$$

$$+ \frac{u_e^2}{T_e}\left[\ell (f_{\eta\eta})^2 + \beta f_\eta \left(\theta - \frac{\rho_e}{\rho}\right)\right] = \frac{\beta}{\frac{du_e}{dx}} \frac{\sum \dot{w}_i h_i}{\rho T_e} \tag{34}$$

The thermodynamic properties and transport coefficients required for definition of the physical problem include a specific heat, an enthalpy, a coefficient of viscosity and a self diffusion coefficient for each of the n pure species present in the boundary layer. In addition, $\frac{n^2-n}{2}$ symmetric binary diffusion coefficents are required to represent the transport interactions between unlike pairs of particles.

The transport properties may be calculated from the following equations (Ref. 23)

$$\mu_i = \frac{5}{16} \frac{(\pi M_i \hbar T)^{1/2}}{\pi \sigma_i^2 \Omega_i (2,2)^*} \tag{35}$$

$$\mathcal{D}_{ij} = \frac{3}{16} \frac{(2\pi \hbar^3 T^3 / M_{ij})^{1/2}}{P \pi \sigma_{ij}^2 \Omega_{ij} (1,1)^*} \tag{36}$$

which are the rigorous kinetic theory formulae for the viscosity and the diffusion coefficients respectively. In order to evaluate these properties one requires a knowledge of the collision diameter σ, and the reduced collision integral Ω^*. In the above equations, M_{ij} is the reduced mass of the binary interaction and σ_{ij} is the simple average of the collision diameters for the pure species i and j. A more complete discussion of the transport coefficients is given in the appendix.

With the exception of three chemical species (i.e. C(g), H, H_2) the numerical values for the transport and thermodynamic properties used in this study are given in references 25 and 26. The thermodynamic properties for carbon gas were obtained from reference 27, while reference 28 supplied the thermodynamic data for the hydrogen system. The transport coefficents for these three species were calculated

using equations 35 and 36. The interactions involving carbon gas were assumed to follow a rigid sphere potential and the collision diameter for this atom was taken to be 3.42 A. The Leonard-Jones 6 - 12 potential function was assumed applicable for the hydrogen system. The potential parameter (i.e. ϵ/k) for this binary encounter (i.e. $H\text{-}H_2$) is 38°K and the collision diameters of the atomic and molecular species are 3.38 A respectively. (Ref. 23, 29). To summarize then, with the exception of hydrogen, all molecule -molecule interactions are based on the use of the Lennard-Jones 6:12 potential, whereas all atom-atom and atom-molecule interactions are based on a rigid sphere potential.

The boundary conditions on the velocity and temperature as applied to the non-dimensional boundary layer equations (eq.. 32-34) are now written. At the surface, the "no slip" condition gives a zero tangential component of velocity.

$$f_{\eta_w} = \frac{u_w}{u_e} = 0 \tag{37}$$

In the absence of mass injection or suction, the normal component of velocity vanishes, hence,

$$-f_w = \frac{\dot{m}_w}{\left[\rho_w \mu_w \frac{du_e}{dx}/\beta\right]^{1/2}} = 0 \tag{38}$$

and the non-dimensional surface temperature becomes

$$\theta_w = \frac{T_w}{T_e} \tag{39}$$

The boundary conditions at the outer edge of the boundary layer for velocity and temperature are given by:

$$\lim_{\eta \to \infty} f_\eta = \lim_{\eta \to \infty} \theta = 1.0 \tag{40}$$

In addition to these usual boundary conditions imposed on the temperature and velocity, one must be concerned with the proper chemical constraints on this system of equations. In the ensuing discussion, it will be assumed that the local state of the gas composition within the viscous layer is one of thermochemical equilibrium. The analysis follows the same general format as given in the preceding section. For generality, let us consider an n component C-O-N gas system.

At the outer edge of the boundary layer the temperature, pressure, enthalpy, etc. are determined by the methods described earlier (i.e. a normal shock computation followed by an isentropic compression). The chemical composition at the edge of the viscous layer is, of course, available as a result of this solution.

Now, within the viscous layer, where diffusion effects cannot be neglected, the lighter-weight particles tend to diffuse faster than the heavier ones which results in preferential diffusion. Because of this, the k-1 relationships for the conservation of chemical elements will not be in the form of mass balance ratios (eq. 6). Instead, constraints are placed on the chemical source terms ($\dot{w}_i$) appearing in equations 32 and 34. Since the masses of the indivudual chemical elements must be conserved, one may write for the C-O-N system:

$$\dot{W}_{\widetilde{O}} = 0; \quad \dot{W}_{\widetilde{N}} = 0 \tag{41}$$

The conservation of mass of the element oxygen is written as follows:

$$\dot{W}_{\widetilde{O}} = \dot{W}_O + \dot{W}_{O_2} + \mathcal{M}_O \sum_i \left(\frac{\dot{W}_i}{\mathcal{M}_i}\right)_O + \mathcal{M}_{O_2} \sum_{j \neq i} \left(\frac{\dot{W}_j}{\mathcal{M}_j}\right)_{O_2} \tag{42}$$

The interpretation of the above expression is similar to that of equation 7.

For the overall conservation of mass, one has

$$\sum_i \dot{W}_i = 0 \tag{43}$$

It is obvious that equations 41 and 43 together imply that the mass rate of formation of the element carbon is also zero.

To complete the analysis of the gas phase chemistry, it is noted that n - k relationships are still needed which specify the rates of the chemical reactions. From the assumption of local thermochemical equilibrium, one has the necessary information from the n - k equilibrium functions, in the form of equation 10.

In this study, it was not found necessary to consider either catalytic or non-catalytic effects of the surface on the boundary layer chemistry because of the initial assumption of local thermochemical equilibrium through the gas layer. Although real engineering surfaces have finite catalytic efficiency, since the gas is already assumed to be in an equilibrium state, the chemical activity of the surface can in no way influence the gas state without producing a departure from equilibrium in the gas phase. It is usually under conditions of low density (i.e., the low Reynolds number regime) where the influence of finite catalytic efficiency is observed, because in this case, the free stream gas is not initially in a state of thermochemical equilibrium as it enters the low density viscous layer. Only the high Reynolds number problem has been treated here.

In the absence of mass transfer (transpiration cooling or ablation), the net mass flux at the surface must be zero. This means that the net mass flux of the k chemical elements must separately vanish at the surface. One is free to specify k-1 such relationships as follows:

$$\left(\dot{m}_{\widetilde{O}}\right)_W = 0 \; ; \; \left(\dot{m}_{\widetilde{N}}\right)_W = 0 \tag{44}$$

The net mass flux of the element oxygen for example, is defined to be:

$$\left(\dot{m}_{\widetilde{O}}\right)_w = \left[\dot{m}_O + \dot{m}_{O_2} + \mathcal{M}_O \sum_i \left(\frac{\dot{m}_i}{\mathcal{M}_i}\right)_O + \mathcal{M}_{O_2} \sum_{j \neq i} \left(\frac{\dot{m}_j}{\mathcal{M}_j}\right)_{O_2}\right]_w \tag{45}$$

To complete the system, one makes use of Dalton's Law (eq. 9) and the n - k equilibrium K_p functions.

DISCUSSIONS OF NUMERICAL RESULTS

a) Thermochemistry and Boundary Layer Profiles.

Comparisons of some of the thermochemical properties and compositions of the various gas systems are presented in figure 2 through 5 and in Table I. Figure 2 shows the enthalpies of the pure chemical species as a function of temperature. The reference temperature of 536.7°R has been selected for these calculations, and the enthalpies of H_2, N_2, and O_2 molecules in their standard state are taken to be zero at this temperature, in agreement with customary thermodynamical definitions. The enthalpy of the hydrogen atom (not included in figure 2) was based on a heat of formation of 93,762 BTU/LB. and a specific heat of 4.97 BTU/LB. °R. It is also noted that the enthalpies of formation of carbon monoxide and carbon dioxide are negative with respect to the major components of air, (see Table II).

The equilibrium dissociation levels of the three diatomic gases treated are shown in figure 3 as a function of temperature at a pressure level equal to one standard earth atmosphere. These were based on the equilibrium constants given in Table III. A comparison of the gases indicates that the equilibrium dissociation levels of oxygen and hydrogen are nearly the same function of temperature. Nitrogen, on the other hand, has a dissociation energy per mole approximately twice that of oxygen and hydrogen and consequently its dissociation occurs at correspondingly high gas temperatures.

The equilibrium chemistry in terms of mole fractions of the carbon dioxide gas system is seen in figure 4. Three regimes of chemical activity are apparent. At the lower temperatures, carbon dioxide is dissociating to form carbon monoxide and molecular oxygen in accordance with the following reaction:

$$CO_2 \rightleftharpoons CO + 1/2\ O_2$$

At slightly higher temperatures, and before the above reaction has gone to completion, the oxygen molecule dissociates, (i.e. $O_2 \rightarrow 2O$). At the highest temperatures, the carbon monoxide breaks down to form atomic gaseous carbon and additional atomic oxygen. The mean molecular weight of this system therefore ranges from its low temperature value of 44 LB/LB.-mole to 14.67 LB/LB-mole for complete dissociation. The magnitude of the enthalpy of this gas ranges from -3850 BTU/LB at the reference temperature to over 17,000 BTU/LB at a temperature of 16,000 °R. The resulting overall enthalpy change is nearly 21,000 BTU/LB which is approximately twice the enthalpy change for air over the same range of temperature. This would imply that in a carbon dioxide atmosphere, higher flight velocities may be sustained (than in air, say) before appreciable ionization levels would be encountered.

Figure 5 shows two gas models which may be used to simulate the air system. The four component model includes molecular and atomic oxygen and nitrogen, while the five component model introduces the additional species nitric oxide. It is found that the four component model shown in figure 5 is entirely adequate for simulating the energy content of high temperature air over a wide range of altitudes and flight speeds.

The normal shock and isentropic compression calculations provide another means for comparison of the different gas systems. Numerical results of a representative set of normal shock and stagnation point computations are shown in Table I. Note that the three ambient conditions (i.e. flight velocity, temperature, and pressure) are fixed for all of the gas systems. The free stream density, therefore, increases as the mean molecular weight of the gas system. The free stream enthalpy is seen to be a direct function of the enthalpies of formation of the gases comprising each system.

Consider next in Table I the temperature (T_2) immediately behind the normal shock. Since the hydrogen system has a large heat capacity and an enormous enthalpy

of formation for atomic hydrogen, it is not surprising to find a low shock temperature with an associated low dissociation level. The nitrogen, air and carbon dioxide systems are found to have very nearly equivalent shock temperatures. However, the oxygen system, due to the relatively lower dissociation energy of the oxygen molecule, is found to be completely dissociated for this flight condition, and consequently gives rise to a higher shock temperature. The shock pressure P_2 is found to increase with increasing molecular weight of the particular gas system. This is expected from the free stream density variation with molecular weight. Referring to equation 3 and utilizing the hypersonic approximation, one has

$$P_2 \approx \rho_\infty V_\infty^2 \tag{46}$$

and then introducing the equation of state (5), one obtains

$$P_2 \approx \frac{P_\infty \bar{m}_\infty}{\mathcal{R} T_\infty} V_\infty^2 \tag{47}$$

Hence, for the same initial free stream conditions of pressure P_∞, and temperature T_∞, and flight speed V_∞, the shock pressure P_2 is directly proportional to the mean molecular weight of the ambient gas. For those gases for which T_2 is nearly the same, the density ρ_2 behind the normal shock has, in general, the same variation with free stream molecular weight as does the shock pressure. However, we note that since the oxygen system is completely dissociated, its gas density is slightly lower than that of the air or nitrogen systems. One notes further that the enthalpies h_2 of hydrogen, nitrogen, air and oxygen are approximately the same. However, the enthalpy of the carbon dioxide system is substantially lower due to its negative heat of formation. The absolute level of the enthalpies (i.e. h_∞, h_2, h_e) for all gas systems will be dependent upon the selection of a particular reference temperature. However, the enthalpy changes and the other thermodynamic quantities (i.e. T, P. ρ, $\bar{m}$) are quite independent of any arbitrary selection of the reference temperature.

The stagnation region values of temperature, pressure, density and enthalpy are seen to increase slightly over their normal shock values. However, the composition of the gas, as reflected by its mean molecular weight, has not changed significantly during the isentropic compression process. The stagnation point velocity gradient, given in Table I, was calculated following the modified Newtonian theory. The percent dissociation tabulated for each of the gases was based on the minimum mean molecular weight possible for each dissociated system and was calculated by the following equation:

$$\% \text{ Dissociation} = \frac{\bar{m}_\infty - \bar{m}_e}{\bar{m}_\infty - \bar{m}_{min.}} \times 100 \qquad (48)$$

If one had chosen to compare the various gas systems on the basis of a constant free stream density instead of a constant free stream pressure as indicated in Table I, then equation 46 shows that the stagnation pressures of all the gases will be identical for the flight speed considered. Equation 4 indicates that the stagnation enthalpies would be the same as those listed in Table I. Examination of equation 12 and 13 and figure 2 reveals that the equilibrium shock temperature of the carbon dioxide mixtures will be less than that for air, oxygen or nitrogen. However, examination of the equation of state for these conditions reveals that the shock density of pure carbon dioxide will still be greater than that for air.

In general, the state of a gas stream is completely defined by two independent thermodynamic state quantities in addition to the macroscopic stream velocity. However, as will be shown later, one may predict the approximate aerodynamic heating rate in any arbitrary gas mixture by specifying only ρ_∞, V_∞ and $\bar{m}_\infty$.

The information contained in figure 6 provides a means of estimating an upper limit on the validity of the gas models considered in this study. The curves of free stream densities versus flight speed indicate a bound on the flight corridor in

which the gases shown are approximately less than one percent ionized, or, to the same order of approximation, less than ninety-nine percent dissociated. Here, we have definite evidence that a carbon dioxide atmosphere can sustain relatively higher flight speeds than the other gases shown before encountering appreciable ionization phenomena. In a pure hydrogen atmosphere, of course, the vehicle can travel at flight velocities in the range of 60 - 70 thousand feet per second before producing dissociation inside the shock layer. It should be noted that the free stream density and flight velocity of one of the cases that has been treated (i.e. oxygen at 24,000 ft./sec., Table I) falls to the right of the appropriate curve in figure 6. However, since the heating rate associated with this gas at this flight condition correlates well (as will be shown later) with the results for the other gases, it is possible that all of the correletions may be valid at higher flight speeds than indicated as figure 6.

In figures 7 and 8 are shown a typical set of numerical solutions that have been obtained on an IBM 7090 digital computer for the boundary layer equations for the dissociating diatomic gases O_2, N_2 and H_2, for a particular set of flight conditions. Figure 7 indicates the variation of gas temperature and tangential gas velocity across the stagnation point boundary layer for a vehicle travelling at 24,000 ft./sec., at an altitude such that the ambient pressure and temperature are 0.472 LB/FT.^{2} and 449°R respectively. The instantaneous surface temperature was taken to be 800°R for all three cases. Figure 8 shows the corresponding variation of gas composition through the layer as a function of η, the non-dimensional distance measured from the surface.

The resulting boundary layer distributions of temperature, tangential velocity and gas composition, in air and carbon dioxide, corresponding to the same gas conditions utilized for the pure diatomic gases, are shown in figures 9 to 11. By way of comparison, results for oxygen and nitrogen are also shown in figure 9. Here, the surface temperature was arbitrarily taken as 3500°R.

It is interesting to observe that whereas figures 8, 10 and 11 present the variation of equilibrium gas composition with distance from the surface in a layer of constant pressure, figures 3, 4 and 5 show the variation of equilibrium gas composition with gas temperature at constant pressure. Since it is seen in figures 5 and 7 that the gas temperature does not vary linearly with distance from the vehicle surface, clearly figures 8, 10 and 11 are essentially distorted versions of a set of curves which would look like figures 3, 4 and 5, if the former were replotted versus gas temperature.

The boundary layer temperature and velocity profiles for a gas mixture composed of 50% nitrogen and 50% carbon dioxide by mass are shown in figure 12. The limiting cases of pure nitrogen and pure carbon dioxide are included for comparison. The variation in gas composition of the nitrogen-carbon dioxide mixture, as a function of the non-dimensional distance within the boundary layer, is shown in figure 13.

Note (see figure 12) that although the velocity profiles for these three cases are similiar, the temperature profiles are quite different. The nitrogen boundary layer is seen here to be characterized by a high temperature gradient at the surface. This is due to the fact that atomic nitrogen recombines at relatively high temperatures within the gas phase and this gas temperature is sustained rather close to the surface. In contrast with this, we note that in the carbon dioxide boundary layer, the chemical reactions (see figure 11) release energy further out in the gas phase, lowering the gas temperature and resulting temperature gradient at the surface. However, as will be shown later, the heat transferred to the surface by a carbon dioxide gas is greater than that transferred by a nitrogen gas (all other conditions being similiar), indicating, that in carbon dioxide, an appreciable amount of energy is transfered to the surface by the diffusion of chemical species, in addition to the energy transfered by conduction.

b) Heat Transfer and Skin Friction Correlations

The aerodynamic heat transfer rate to the surface of the vehicle, in the absence of mass transfer or surface slip is given by:

$$Q_w = \left(K \frac{\partial T}{\partial y} - \sum_i \rho_i V_i h_i \right)_w \tag{49}$$

In terms of the transformed variables, equation (49) becomes, when thermal diffusion is neglected:

$$Q_w = \sqrt{\frac{\rho_w \left(\frac{du_e}{dx}\right)_s}{\mu_w \beta}} \left[K \quad T_e \theta_\eta \quad - \frac{\mu}{Pr} \sum_i \mathcal{M}_i h_i \sum_{j \neq i} \frac{\mathcal{M}_j L_{ij}}{\bar{\mathcal{M}}^2} X_{j\,\eta} \right]_w \tag{50}$$

where the modified Newtonian velocity gradient is given by:

$$\frac{du_e}{dx} = \frac{1}{R_B} \sqrt{\frac{P_e - P_\infty}{\rho_e}} \tag{51}$$

and all other quantities appearing in equation (50) are obtained during the solution of the boundary layer equations.

Upon introducing the following definitions for the Nusselt number and Reynolds number, based on surface conditions,

$$Nu = \frac{Q_w \bar{C}_{p_w} x}{K_w (H_e - h_w)} \tag{52}$$

and

$$Re_w = \frac{\rho_w u_e x}{\mu_w} \tag{53}$$

one obtains:

$$\frac{Nu}{\sqrt{Re_w}} = \frac{Q_w \bar{C}_{p_w}}{K_w (H_e - h_w)} \sqrt{\frac{x \mu_w}{u_e \rho_w}} \tag{54}$$

where:

$$u_e \approx \frac{du_e}{dx} x \tag{55}$$

Two attempts have been made to correlate the effect of molecular weight of the various gas systems upon the dimensionless group $Nu/\sqrt{Re}_w$, and these are shown in figures 14 and 15. When the numerical results from equation (50) are inserted into equation (54) for each of the eight gas systems treated here and these results are plotted versus flight velocity, one obtains the results shown in figure 14. As is shown, this method of correlation might be useful when only a single gas is involved, but when the results of other gases are included, no molecular weight correlation appears. When one plots the dimensionless heat transfer parameter $Nu/\sqrt{Re}_w$ as a logarithmic function of the normalized product of density and viscosity across the boundary layer, one obtains the results shown in figure 15. It is most interesting that a plot of $Nu/\sqrt{Re}_w$ versus $\rho_e \mu_e/\rho_w \mu_w$ collapses the extensive numerical computations since here the effects of molecular weight, although certainly present, are not at all pronounced. It is the opinion of the authors that the data presented in figures 14 and 15 is not necessarily in the most useful form and that better methods exist for the correlation of hypersonic heat transfer. These will be shown below.

Earlier work (e.g., Ref 26) on aerodynamic heat transfer at hypersonic speeds suggests that another useful way of correlating the results would be with stagnation enthalpy and stagnation pressure. That is, one finds that the normalized aerodynamic heat transfer parameter $Q_w\sqrt{\frac{R_B}{P_e}}$ is usually a linear function of the enthalpy difference $(H_e - h_w)$ across the boundary layer, and when one plots the numerical results in this manner for the eight gaseous systems treated here, one obtains the results shown in figure 16. Here, the molecular weight effect is most pronounced and is, in fact, separable.

Thus, when one divides the aerodynamic heat transfer parameter $Q_w\sqrt{\frac{R_B}{P_e}}$ by the enthalpy difference $(H_e - h_w)$, and plots this result versus the molecular

weight of the ambient **undisturbed** gas $\bar{m}_\infty$, one obtains the most useful result shown in figure 17. Here, it is seen that a correlation of all the numerical solutions to a high order set of coupled non-linear differential equations, governing the aerodynamic heat transfer in eight different chemically reacting gases, reduces to a single straight line. This straight line can be represented by the equation; (to within ±8%):

$$\frac{Q_w (R_B/P_e)^{1/2}}{H_e - h_w} = (12.0 + 0.866\, \bar{m}_\infty) \times 10^{-3} \qquad (56)$$

where the symbols have the following meaning and physical dimensions.

Q_w - heat transfer rate, $\frac{BTU}{ft.^2 sec.}$

R_B - vehicle nose radius, ft.

P_e - stagnation pressure, atm.

$\bar{m}_\infty$ - molecular weight of ambient gas

H_e - stagnation enthalpy, BTU/lb.

h_w - static enthalpy of gas mixture evaluated at surface temperature, BTU/lb.

The results of other theoretical and experimental studies pertaining to hypersonic stagnation point heat transfer in several different gas mixtures are also included in figure 17. Item 6 on figure 17 indicates the range of the correlated theoretical heat transfer parameter in air and is explained in greater detail in table IV. Hoshizaki's theoretical results for CO_2 are seen to fall slightly below the theoretical prediction of this present study. However, it is noted that there is favorable agreement between the various theoretical studies and experimental results.

Returning to equation (1), we are now in a position to relate the coefficient C to the first term on the right hand side of equation (56). We introduce the two hypersonic approximations

$$P_e \approx \rho_\infty V_\infty^2 \tag{57}$$

$$H_e - h_w \approx \frac{V_\infty^2}{2} \tag{58}$$

into equation (1) and we obtain

$$C = \frac{Q_w \sqrt{R_B}}{\sqrt{\rho_\infty}\ V_\infty^3} \approx \frac{Q_w \sqrt{\frac{R_B}{P_e}}}{2(H_e - h_w)} \tag{59}$$

where appropriate physical dimensions must be utilized in equation (59). Thus, for example, if one writes:

$$Q_w = 2C\,(H_e - h_w)\sqrt{\frac{P_e}{R_B}} \tag{60}$$

where all of the physical quantities in equation (60) have been defined immediately following equation (56), then one has:

$$C = (6.0 + 0.433\,\bar{m}_\infty) \times 10^{-3},\ \frac{\text{lb.}}{\text{ft.}^{3/2}\,\text{sec.}\ \text{atm.}^{1/2}} \tag{61}$$

On the other hand, if one writes:

$$Q_w = \frac{C}{\sqrt{R_B}}\sqrt{\rho_\infty}\ V_\infty^3 \tag{1}$$

where the physical quantities have dimensions given by:

ρ_∞ - ambient density, lb./ft.^{3}

R_B - nose radius, ft.

V_∞ - flight speed, ft./sec.

then the coefficient C has the value:

$$C = (9.18 + 0.663\,\bar{m}_\infty) \times 10^{-10},\ \frac{\text{BTU sec.}^2}{\text{ft.}^3\ \text{lb}^{1/2}} \tag{62}$$

Note that although equation (56) as written, applies specifically at the axi-symmetric stagnation point of a body in a hypersonic stream, the result is actually considerably more general since one anticipates that

$$\frac{Q_w \sqrt{2R}_B}{P_e^{1/2} f(\Lambda)} \left[\frac{f(\Lambda)}{\sqrt{2}}\right]^{\delta} = (12 + 0.866 \bar{m}_\infty) \times 10^{-3} (H_e - h_w) \qquad (63)$$

which applies over both two-dimensional (cylindrical) and axi-symmetric shapes including the effects of yaw, where the additional terms are defined as follows:

δ is the Kroncker delta such that

$$\begin{cases} \delta = 1: & \text{(axi-symmetric shapes)} \\ \delta = 0: & \text{(two-dimensional shapes)} \end{cases} \qquad (64)$$

P_e is the local static pressure at the outer edge of the boundary layer expressed in atmospheres, H_e is the stagnation enthalpy in BTU/lb., and **h_w is the local wall gas enthalpy in BTU/lb., and $f(\Lambda)$ represents the effects of yaw and may be written:**

$$f(\Lambda) = \cos^{3/2} \Lambda \qquad (65)$$

to a good first approximation if the surface temperature remains relatively cool, (ref. 30).

For a modified Newtonian pressure distribution

$$P_e = P_{e_s} \cos^2 \varphi + P_\infty \sin^2 \varphi \qquad (66)$$

and hence over the forward portion of the body where the first term on the right dominates, the heat transfer rate will decrease as one proceeds away from the forward stagnation point at a rate directly proportional to $\cos \varphi$.

It is noted, in passing, that for the same ambient conditions of density (ρ_∞) and flight velocity (V_∞) the heat transfer rate in pure carbon dioxide is 36% larger than in air. However, in a test facility, in which one may have greater control over T_∞, P_∞ and V_∞ say, or in flight for which T_∞, P_∞, and V_∞ are fixed, then the heat

transfer in a pure carbon dioxide atmosphere is 68% larger than in air, since for this situation the molecular weight effect shows up twice.

Upon introducing the definition of the Stanton number and the shock Reynolds number

$$C_H = \frac{Q_w}{\rho_\infty V_\infty (H_e - h_w)} \tag{67}$$

$$Re_s = \frac{\rho_\infty V_\infty R_B}{\mu_e} \tag{68}$$

one obtains:

$$C_H \sqrt{Re_s} = \frac{Q_w}{\sqrt{\rho_\infty V_\infty} (H_e - h_w)} \sqrt{\frac{R_B}{\mu_e}} \tag{69}$$

The skin friction coefficient may be defined as

$$C_f = \frac{\tau_w}{1/2\, \rho_\infty V_\infty^2} \tag{70}$$

where the aerodynamic shear stress at the surface of the vehicle is given as

$$\tau_w = \mu_w \left(\frac{\partial u}{\partial y}\right)_w = \left(\frac{\rho_w \mu_w \frac{du_e}{dx}}{\beta}\right)^{1/2} u_e f_{\eta\eta_w} \tag{71}$$

Hence, one also obtains:

$$2\, C_H/C_f = \frac{Q_w}{(H_e - h_w)} \frac{V_\infty}{\tau_w} \tag{72}$$

Upon calculating the quantities $C_H \sqrt{Re_s}$ and $\left(\frac{2C_H}{C_f}\right)\left(\frac{x}{R_B}\right)$ for all of the gaseous systems and plotting the results versus the quantity $V_\infty / R_B \left(\frac{du_e}{dx}\right)_s$, one obtains a set of straight line correlations (see figure 18). It appears that one can therefore write:

$$C_H \sqrt{Re_s} \approx \frac{V_\infty}{R_B \left(\frac{du_e}{dx}\right)_s} \tag{73}$$

and

$$\left(\frac{2C_H}{C_f}\right)\left(\frac{x}{R_B}\right) \approx -0.6 + C_H \sqrt{Re_s} \tag{74}$$

It is noted that Reynolds' analogy states that

$$\left(\frac{Q}{\tau}\right)_w = \left(\frac{K\frac{\partial T}{\partial y}}{\mu\frac{\partial u}{\partial y}}\right)_w \cong \frac{K_w(T_e-T_w)}{\mu_w(u_e-u_w)} \cong \frac{h_e-h_w}{Pr_w\, u_e} \tag{75}$$

substituting equation (75) into equation (72) and using the relationship for the velocity given in equation (55) one obtains

$$\left(\frac{2C_H}{C_f}\right)\left(\frac{x}{R_B}\right) = \frac{V_\infty}{Pr_w\, R_B\left(\frac{du_e}{dx}\right)_s} \tag{76}$$

Clearly then, the results of figure 18 would appear to indicate that Reynolds' analogy applies to the same degree of accuracy as the Prandtl number of the various gases differs from unity. In figure 19 it is seen that the theoretically determined Prandtl number for a wide range of gases, lies in the range $0.62 \leq Pr \leq 0.74$.

CONCLUSIONS

In this study of the aerodynamic laminar stagnation region heat transfer in eight different dissociating gas mixtures, a correlation of all of the numerical results to a high order set of coupled non-linear differential equations yielded a single straight line representation. That is, it was found that the aerodynamic heat transfer parameter $Q_w\sqrt{\frac{R_B}{P_e}}$ is directly proportional to the enthalpy difference (H_e-h_w) for each of the eight gases treated. Moreover, when the effects of molecular weight were correlated, it was found that the aerodynamic stagnation point heat transfer parameter correlates linearly with the molecular weight of the undisturbed gas in the following manner.

$$\frac{Q_w\sqrt{R_B}}{\sqrt{P_e}\,(H_e-h_w)} = (12.0 + 0.866\,\bar{m}_\infty) \times 10^{-3}, \quad \frac{\text{lb.}}{\text{ft.}^{3/2}\,\text{sec.}\,\text{atm.}^{1/2}} \tag{77}$$

It was also found possible to correlate the skin friction coefficient C_f for the eight gases treated, and it was shown that Reynolds' analogy provides a reasonable representation of the ratio of heat transfer to skin friction.

The results obtained here apply over a wide range of hypersonic flight speeds. Since more energy is required in order to dissociate CO_2 and H_2 than air, the results apply directly at considerably higher flight speeds in a pure hydrogen atmosphere and at somewhat higher flight speeds in a pure carbon dioxide atmosphere than in Earth's atmosphere. It is expected that the results may also apply to the complex aerothermochemical environment produced by the gases flowing out of a rocket motor over a test model.

ACKNOWLEDGMENTS

The numerical results were obtained on an IBM 7090 digital computer by Mr. Frank Bosworth who programmed the governing equations.

This study was supported in part by the Jet Propulsion Laboratory, California Institute of Technology under subcontract 950250 sponsored by the National Aeronautics and Space Administration via contract NAS 7-100, and in part by the General Electric Company under its Contractor's Independent Research and Development Program.

APPENDIX

The transport properties can be described by the distribution function $f_i^{(1)}(r, P, t)$ which is the solution of the well known Maxwell-Boltzmann integro-differential equation.

$$\frac{\partial f_i^{(1)}}{\partial t} + \frac{1}{m_i}\left(\vec{P}_i \frac{\partial f_i^{(1)}}{\partial r} + \vec{X}_i \frac{\partial f_i^{(1)}}{\partial P_i}\right) = \sum_j \left(\Gamma_{ij}^{(+)} - \Gamma_{ij}^{(-)}\right) \qquad \text{(A1)}$$

The right hand side of eq. A1 accounts for the collision processes occurring between the components of the system. The Maxwell-Boltzmann equation may be solved by means of the Enskog perturbation technique, which ultimately reduces the equations to linear integrals and finally to a set of linear algebraic equations. Chapman and Cowling (Ref. 31) and Hirschfelder, Curtiss and Bird (Ref. 23) have shown that the

coefficients of these algebraic equations may be expressed in terms of the definite integrals, $\Omega(\ell, s)$. Recently, Cohen, Spitzer and Routly (Ref. 32), derived a modified equation which they considered more appropriate for inverse square forces, and treated the distant encounters by means of the Fokker-Planck equation.

Following the Hirschfelder, Curtiss and Bird technique (Ref. 23) the omega integrals, from which the various transport coefficients may be computed, are expressed as:

$$\Omega_{ij} = \sqrt{\frac{2\pi\hbar T}{m_{ij}}} \int_0^\infty \int_0^\infty e^{-v^2} e^{2s+3} (1 - \cos^\ell \chi) \, dbdV \tag{A2}$$

$$\Omega^{(\ell, s)} = \sqrt{\frac{\hbar T}{2\pi m_{ij}}} \int_0^\infty e^{-v^2} V^{2s+3} Q^{(\ell)}(g) \, dV \tag{A3}$$

where the angle of deflection χ is a function of the relative velocity (g) and the impact parameter (b) expressed as:

$$\chi(g, b) = \pi - 2b \int_{r_m}^\infty r^2 \sqrt{1 - \frac{b^2}{r^2} - \frac{2\phi(r)}{m_{ij} g^2}}} \tag{A4}$$

where r_m is the lowest root for which the radical in the integrand vanishes. The cross section (Q) is

$$Q^{(\ell)}(g) = 2\pi \int_0^\infty (1 - \cos^\ell \chi) \, bdb \tag{A5}$$

The transport properties of the pure species may be calculated from the following equations.

$$\mu_i = \frac{5}{16} \frac{(\pi M_i \hbar T)^{1/2}}{\pi \sigma_i^2 \Omega_i^{(2,2)*}} \tag{A6}$$

$$\mathcal{D}_{ij} = \frac{3}{16} \frac{\left(2\pi\hbar^3 T^3 / M_{ij}\right)^{1/2}}{P\pi\sigma_{ij}^2 \Omega_{ij}^{(1,1)*}} \tag{A7}$$

which are the rigorous kinetic theory formulae for the viscosity and the binary diffusion coefficients respectively. Note that the self diffusion coefficients are also obtained from eq. A7 by a proper interpretation of symbols (i.e. $j \equiv i$). In order to calculate these properties one requires a knowledge of the collision diameter σ, and the reduced collision integral Ω^*. In the above equations M_{ij} is the reduced mass of the binary interaction and σ_{ij} is the simple average of the collision diameters for the pure species i and j.

Having a knowledge of the transport properties of the pure species and the composition of a gas mixture, one is then in a position to consider the transport properties of the gas mixture.

The coefficient of viscosity for an n component gas mixture may be written in terms of the mole fractions, the viscosities of the pure species and the binary diffusion coefficients as follows: (Ref. 23)

$$\mu_{mix} = \sum_{i}^{n} \frac{X_i^2}{\frac{X_i^2}{\mu_i} + 1.385 \sum_{j \neq i} \frac{X_i X_j \mathcal{R} T}{P \mathcal{M}_i \mathcal{D}_{ij}}} \tag{A8}$$

Although the binary diffusion coefficients are symmetric (i.e., $\mathcal{D}_{ij} \equiv \mathcal{D}_{ij}$), the multicomponent diffusion coefficients are not. This is apparent from the following definitions. (Ref. 23):

$$D_{ij} = \frac{\bar{\mathcal{M}}}{\mathcal{M}_j} \frac{\mathcal{K}^{ji} - \mathcal{K}^{ii}}{|\mathcal{K}|} \tag{A9}$$

where:

$$\mathcal{K}^{ji} = (-1)^{i+j} \begin{vmatrix} 0 & \cdots & \mathcal{K}_{1,\,i-1} & \mathcal{K}_{1,\,i+1} & \cdots & \mathcal{K}_{1,\,N} \\ \vdots & & \vdots & \vdots & & \vdots \\ \mathcal{K}_{j-1,\,1} & \cdots & \mathcal{K}_{j-1,\,i-1} & \mathcal{K}_{j-1,\,i+1} & \cdots & \mathcal{K}_{j-1,\,N} \\ \mathcal{K}_{j+1,\,1} & \cdots & \mathcal{K}_{j+1,\,i-1} & \mathcal{K}_{j+1,\,i+1} & \cdots & \mathcal{K}_{j+1,\,N} \\ \vdots & & \vdots & \vdots & & \vdots \\ \mathcal{K}_{N,\,1} & \cdots & \mathcal{K}_{N,\,i-1} & \mathcal{K}_{N,\,i+1} & \cdots & \mathcal{K}_{N,\,N} \end{vmatrix} \tag{A10}$$

in the above $K_{ii} = 0$ and

$$\mathcal{K}_{i,j} = \frac{X_i}{\mathcal{D}_{ij}} + \frac{\mathcal{M}_j}{\mathcal{M}_i} \sum_{k \neq i} \frac{X_k}{\mathcal{D}_{ik}} \tag{A11}$$

The frozen thermal conductivity of the mixture with the Eucken correction is given by (Ref. 33)

$$K_{mix.}^{Eucken} = K_{mix.} + \sum_{i}^{n} X_i \frac{K_i^{Eucken} - K_i}{\sum_{j}^{n} X_j \frac{\mathcal{D}_{ii}}{\mathcal{D}_{ij}}} \tag{A12}$$

$K_{Mix.}$ is defined by the following

$$K_{Mix.} = \frac{\begin{vmatrix} \mathcal{L}_{ii}^{11} & \cdots & \mathcal{L}_{in}^{11} & X_1 \\ \vdots & & \vdots & \vdots \\ \mathcal{L}_{ni}^{11} & \cdots & \mathcal{L}_{nn}^{11} & X_n \\ X_i & \cdots & X_n & 0 \end{vmatrix}}{\begin{vmatrix} \mathcal{L}_{ii}^{11} & \cdots & \mathcal{L}_{in}^{11} \\ \vdots & & \vdots \\ \mathcal{L}_{ni}^{11} & \cdots & \mathcal{L}_{nn}^{11} \end{vmatrix}} \tag{A13}$$

The elements of the above matrices are

$$\mathcal{L}_{ii}^{11} = -\frac{4X_i^2}{K_i} - \frac{16T}{25P} \sum_{j \neq i} \frac{X_i X_k \left[\frac{15}{2}\mathcal{M}_i^2 + \frac{25}{4}\mathcal{M}_k^2 - 3\mathcal{M}_k^2 B_{ik}^* + 4\mathcal{M}_i \mathcal{M}_k A_{ik}^*\right]}{(\mathcal{M}_i + \mathcal{M}_k)^2 \mathcal{D}_{ik}} \tag{A14}$$

and

$$\mathcal{L}_{ij}^{11} = \frac{16T}{25P} \frac{X_i X_j \mathcal{M}_i \mathcal{M}_j}{(\mathcal{M}_i + \mathcal{M}_j)^2 \mathcal{D}_{ij}} \left[\frac{55}{4} - 3B_{ij}^* - 4A_{ij}^*\right] \tag{A15}$$

The thermal conductivities of the pure species are given in terms of viscosities and specific heats as follows:

$$K_i^{Eucken} = \frac{15}{4}\frac{\mathcal{R}}{\mathcal{M}_i} \mu_i \left(\frac{4}{15}\frac{C_{v_i}}{\mathcal{R}} + \frac{3}{5}\right) \tag{A16}$$

$$K_i = \frac{15}{4} \frac{\Re}{\mathcal{M}_i} \mu_i \tag{A17}$$

The quantities A*, and B* are defined in terms of the reduced omega integrals.

$$A^* = \Omega^{(2,2)*} / \Omega^{(1,1)*} \tag{A18}$$

$$B^* = \frac{5\,\Omega^{(1,2)*} - 4\,\Omega^{(1,3)*}}{\Omega^{(1,1)*}} \tag{A19}$$

One, therefore, observes that in an n component gas there are n values of μ_i, n values of $\mathcal{D}_{ii}$ and $\frac{n^2-n}{2}$ values of $\mathcal{D}_{ij}$. This leads to one viscosity coefficient (μ_{Mix}), one thermal conductivity coefficient ($K^{Eucken}_{Mix.}$) and n^2- n multicomponent diffusion coefficients (D_{ij}). Finally, one is able to define the properties of the fluid mixture in terms of a single Prandtl number ($Pr=\mu_{Mix.}\ \bar{C}_p/K^{Eucken}_{Mix.}$) and n^2- n multicomponent Lewis numbers ($L_{ij}=\rho\bar{C}_p D_{ij}/K^{Eucken}_{Mix.}$). Note that we have utilized the following notation in the main text:

$K \equiv K^{Eucken}_{Mix.}$; $\mu \equiv \mu_{Mix.}$ and $\bar{C}_p \equiv \bar{C}_{p_{Mix.}} = \sum_i C_i C_{p_i}$.

The variation of the Prandtl number with temperature within the boundary layer for the equilibrium dissociated mixtures considered in this study is shown in figure 19. It should be noted that the boundary layer pressure is different for each of the gases shown as indicated in table I. Note also that, since preferential diffusion effects are not neglected in this study, the relative concentrations of the chemical species for a given gas mixture are not always in stochiometric proportions within the viscous layers. The magnitude of this effect may be assessed by comparison of the Prandtl numbers for air, nitrogen and oxygen given in figure 19.

TABLE I

NORMAL SHOCK AND STAGNATION POINT COMPARISONS

V_∞ = 24,000 FT/SEC; T_∞ = 449°R; P_∞ = 0.4715 LB/FT^2; $T_{Ref.}$ = 536.7°R

GAS SYSTEM	H_2	N_2	AIR	O_2	50% N_2 - 50% CO_2	CO_2
$\bar{m}_\infty$, LB/LB-Mole	2.0	28.0	28.9	32.0	34.2	44.0
ρ_∞, LB/FT^3	1.359×10^{-6}	1.903×10^{-5}	1.969×10^{-5}	2.175×10^{-5}	2.330×10^{-5}	2.991×10^{-5}
h_∞, BTU/LB	-3.162×10^{2}	-2.261×10^{1}	-2.167×10^{1}	-1.862×10^{1}	-1.945×10^{3}	-3.868×10^{3}
T_2, °R	3.390×10^{3}	1.181×10^{4}	1.173×10^{4}	1.574×10^{4}	1.218×10^{4}	1.174×10^{4}
P_2, LB/FT^2	2.058×10^{1}	3.210×10^{2}	3.312×10^{2}	3.535×10^{2}	3.929×10^{2}	5.066×10^{2}
ρ_2, LB/FT^3	7.830×10^{-6}	3.217×10^{-4}	3.190×10^{-4}	2.326×10^{-4}	3.932×10^{-4}	5.415×10^{-4}
$\bar{m}_2$, LB/LB-Mole	1.99	18.3	17.4	16.0	18.8	19.5
V_2, FT/SEC	4.166×10^{3}	1.420×10^{3}	1.481×10^{3}	2.245×10^{3}	1.422×10^{3}	1.317×10^{3}
h_2, BTU/LB	1.083×10^{4}	1.143×10^{4}	1.143×10^{4}	1.138×10^{4}	9.522×10^{3}	7.594×10^{3}
T_e, °R	3.455×10^{3}	1.184×10^{4}	1.176×10^{4}	1.606×10^{4}	1.222×10^{4}	1.176×10^{4}
P_e, LB/FT^2	2.277×10^{1}	3.312×10^{2}	3.423×10^{2}	3.719×10^{2}	4.054×10^{2}	5.215×10^{2}
$\bar{m}_e$, LB/LB-Mole	1.99	18.3	17.4	16.0	18.8	19.5
ρ_e, LB/FT^3	8.495×10^{-6}	3.307×10^{-4}	3.283×10^{-4}	2.398×10^{-4}	4.039×10^{-4}	5.593×10^{-4}
h_e, BTU/LB	1.118×10^{4}	1.147×10^{4}	1.147×10^{4}	1.148×10^{4}	9.562×10^{3}	7.628×10^{3}
$R_B\left(\frac{du_e}{dx}\right)_s$ FT/SEC	1.1300×10^{4}	8.022×10^{3}	8.185×10^{3}	9.984×10^{3}	8.032×10^{3}	7.742×10^{3}
% DISSOCIATION	1.0	69.3	79.4	100.0	77.5	83.7

TABLE II

GAS CONSTANTS (*$T_{ref.}$ = 536.7°R.)

Species	σ_i, A	$\mathcal{M}_i$	ϵ /k, °K	ω_e, cm.$^{-1}$	$\Delta h°_{f_i}$ (*) BTU/LB.
H	3.38	1	---	---	93,762
H_2	2.92	2	38.0	4405.	0
O	2.960	16	---	---	6,654
O_2	3.541	32	88.0	1580.4	0
N	2.880	14	---	---	14,527
N_2	3.749	28	79.8	2359.5	0
C	3.42	12	---	---	25,755
CO	3.590	28	110.0	2156.7	-1,698
CO_2	3.897	44	213.0	2349, 1388, 667(2)	-3,848

TABLE III

EQUILIBRIUM CONSTANTS, $\log_{10} K_p = a - b/T(°R)$

Reaction	Equilibrium Constant (P_i is in atm.)	a	b x 10^{-4}
$H_2 \rightleftharpoons 2H$	$K_{P_H} = (P_H)^2/P_{H_2}$	6.38	4.32
$O_2 \rightleftharpoons 2O$	$K_{P_O} = (P_O)^2/P_{O_2}$	6.80	4.68
$N_2 \rightleftharpoons 2N$	$K_{P_N} = (P_N)^2/P_{N_2}$	7.00	9.00
$CO + O \rightleftharpoons CO_2$	$K_{P_{CO_2}} = P_{CO_2}/P_{CO}P_O$	-8.00	-5.04
$C(g) + O \rightleftharpoons CO$	$K_{P_{CO}} = P_{CO}/P_{C(g)}P_O$	-7.43	-10.29

Based on data appearing in:

B. Lewis and G. vonElbe, "Combustion, Flames and Explosions of Gases", Academic Press, New York, 1951.

TABLE IV

COMPARISON OF CORRELATED THEORETICAL HEAT

TRANSFER PARAMETERS IN AIR

(calculations based on data appearing in ref. 5 below)

INVESTIGATORS	Reference	$\frac{Q_w(R_B/P_e)^{1/2}}{(H_e - H_w)}$, $\frac{LB}{FT^{3/2}\ SEC\ ATM^{1/2}}$
SIBULKIN	(1)	0.034 - 0.042
LEES	(2)	0.033 - 0.037
ROMIG	(3)	0.036 - 0.046
FAY & RIDDELL (Le = 1.0)	(4)	0.040 - 0.043
FAY & RIDDELL (Le = 1.4)	(4)	0.045 - 0.047
SCALA & BAULKNIGHT	(5)	0.035 - 0.043

REFERENCES

1. Sibulkin, M., "Heat Transfer Near the Forward Stagnation Point of a Body of Revolution", J. Aeron. Sci., Vol. 19, No. 8, pp. 570-571, August 1952.

2. Lees, L., "Laminar Heat Transfer Over Blunt-Nosed Bodies of Revolution at Hypersonic Flight Speeds", Jet Propulsion, Vol. 26, No. 4, pp. 259-269, April 1956.

3. Romig, M. F., "Stagnation Point Heat Transfer for Hypersonic Flow", Jet Propulsion, Vol. 26, No. 12, pp. 1098-1101, December 1956. Addendum, Vol. 27, No. 12, p. 1255, December 1957.

4. Fay, J. A. and Riddell, F. R., "Theory of Stagnation Point Heat Transfer in Dissociated Air", J. Aeron. Sci., Vol. 25, No. 2, pp. 73-85, February 1958.

5. Scala, S. M. and Baulknight, C. W., "Transport and Thermodynamic Properties in a Hypersonic Laminar Boundary Layer, Part 2 - Applications", ARS Journal, Vol. 30, No. 4, pp. 329-336, April 1960.

6. Gazley, D., Jr., "Deceleration and Heating of a Body Entering a Planetary Atmosphere from Space", Rand Corporation Report P-955, February 1957.

7. Chapman, D. R., "An Approximate Analytical Method for Studying Entry into Planetary Atmospheres", NACA TN 4276, May 1958.

8. Lees, L., Space Technology, Ed., H. S. Seifert, Chapt. 12, p. 12-07, New York, J. Wiley and Sons, 1959.

9. Eggers, A. J. and Wong, T. J., "Motion and Heating During Atmospheric Entry", ARS Preprint 1675-61, April 1961.

10. Hoshizaki, H., "Heat Transfer in Planetary Atmospheres at Super-Satellite Speeds", ARS Journal, Vol. 32, No. 10, pp. 1544-1552, October 1962.

11. Hirschfelder, J. O., "Heat Transfer in Chemically Reacting Mixtures, I", J. Chem. Phys., 26, pp. 274-285, 1957.

12. Hansen, C. F., "Approximations for the Thermodynamic and Transport Properties of High-Temperature Air", NASA TR R-50, 1959.

13. Thomas, M., "The High Temperature Transport Properties of Carbon Dioxide", Douglas Aircraft Co., SM-37790, July 1960.

14. Rutowski, R. W. and Chan, K. K., "Shock Tube Experiments Simulating Entry into Planetary Atmospheres", General Research in Flight Sciences, Vol. I, Part II, Fluid Mechanics, Lockheed Aircraft Corporation Tech. Rept. LMSD-288139, January 1960.

15. Warren, W. R. and Gruszczynski, J. S., "Experimental Planetary Entry for Mars and Venus - 1962, Section III - 3", Ed., K. T. Pugmire, General Electric Company, MSD, TIS R62SD84, October 1962.

16. Yee, L., Bailey, H. E. and Woodward, H. T., "Ballistic Range Measurements of Stagnation Point Heat Transfer in Air and Carbon Dioxide at Velocities up to 18,000 Ft./Sec.", NASA TN D-777, March 1961.

17. Feldman, S., "Hypersonic Gas Dynamic Charts for Equilibrium Air", Avco-Everett Research Laboratory Rept. No. 40, January 1957.

18. McKowen, P., "The Equilibrium Composition and Flow Variables for Air Dissociated by a Strong Shock Wave", Bell Aircraft Corporation Rept. No. 02-984-040, March 1957.

19. Huber, P. W., "Tables and Graphs of Normal Shock Parameters at Hypersonic Mach Numbers and Selected Altitudes", NACA TN 4352, September 1958.

20. Woodward, H. T., "Thermodynamic Properties of Carbon Dioxide and Nitrogen Mixtures Behind a Normal Shock Wave", NASA TN D-1553, 1963.

21. Wittliff, C. E. and Curtis, J. T., "Normal Shock Wave Parameters in Equilibrium Air", Cornell Aeronautical Laboratory Report No. CAL-111, November 1961.

22. Cook, C. A., Gilbert, L. M. and Scala, S. M., "Normal Shock Wave Calculations in Air at Flight Speeds up to 25,000 Ft./Sec.", MSD, General Electric Company, Space Sciences Laboratory, TIS R62SD76, November 1, 1962.

23. Hirschfelder, J. O., Curtiss, C. F. and Bird, R. B., Molecular Theory of Gases and Liquids, John Wiley and Sons, 1954.

24. Scala, S. M., "The Equations of Motion in a Multicomponent Chemically Reacting Gas", General Electric Company, MSD, Space Sciences Laboratory, TIS R58SD205, December 1957.

25. Scala, S. M. and Baulknight, C. W., "Transport and Thermodynamic Properties in the Hypersonic Laminary Boundary Layer, Part 1", ARS Journal, Vol. 29, No. 1, pp. 39-45, January 1959.

26. Scala, S. M., "The Ablation of Graphite in Dissociated Air, Part I - Theory", IAS Paper No. 62-154, Thirtieth National Summer Meeting, June 1962.

27. Browne, W. G., "Thermodynamic Properties of Some Atoms and Atomic Ions", Engineering Physics Technical Memorandum No. 2, General Electric Company, Missile and Space Division, December 1961.

28. Gordon, J., "Thermodynamics of High Temperature Gas Mixtures, and Applications to Combustion Problems", WADC Tech. Rept. 57-33, ASTIA No. 110735, January 1957.

29. Hirschfelder, J. O. and Eliason, M. A., "The Estimation of the Transport Properties for Electronically Excited Atoms and Molecules", University of Wisconsin Technical Report, WIS-AF-1, May 1956.

30. Eggers, A. J., Jr., Hansen, C. F. and Cunningham, B. E., "Stagnation Point Heat Transfer to Blunt Shapes in Hypersonic Flight, Including Effects of Yaw", NACA TN 4229, 1958

31. Chapman, S. and Cowling, T. G., The Mathematical Theory of Non-Uniform Gases, Cambridge University Press, 1939.

32. Cohen, R., Spitzer, L. and Routly, R., "The Electrical Conductivity of an Ionized Gas", Phys. Rev., Vol. 80, p. 230, 1950.

33. Curtiss, C., Private communication.

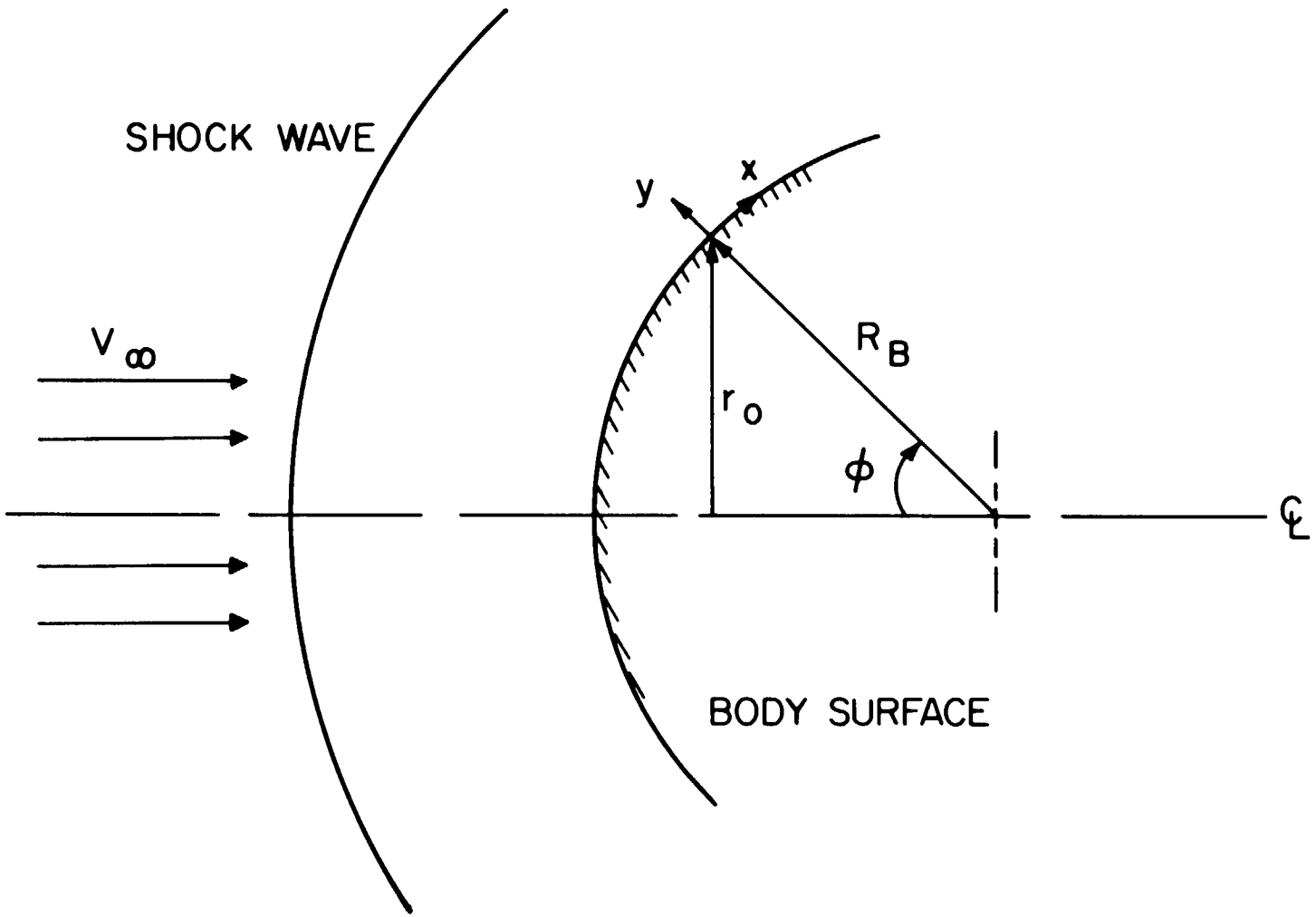

Figure 1. Coordinate System

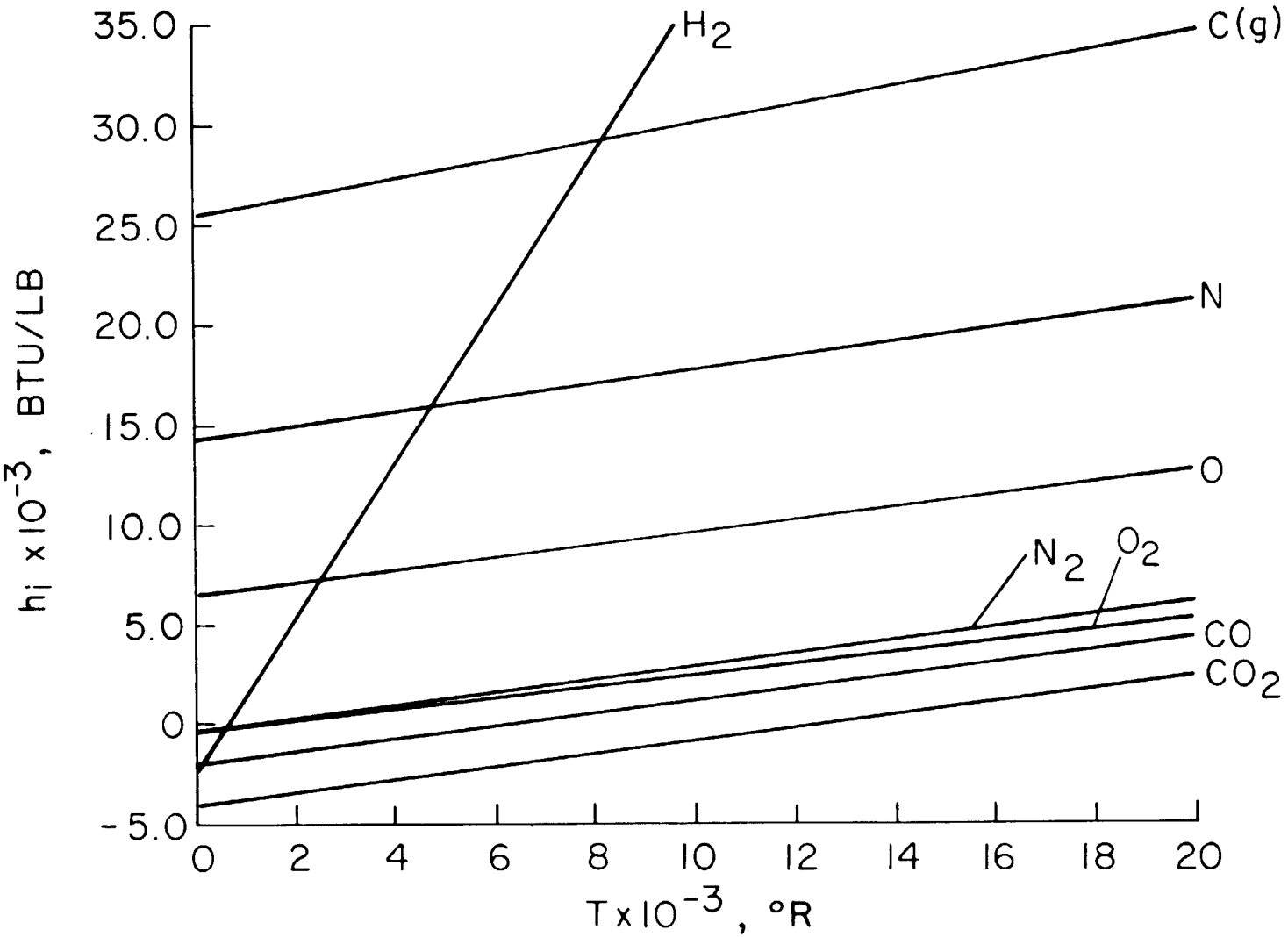

Figure 2. Enthalpy of the Pure Species vs. Temperature

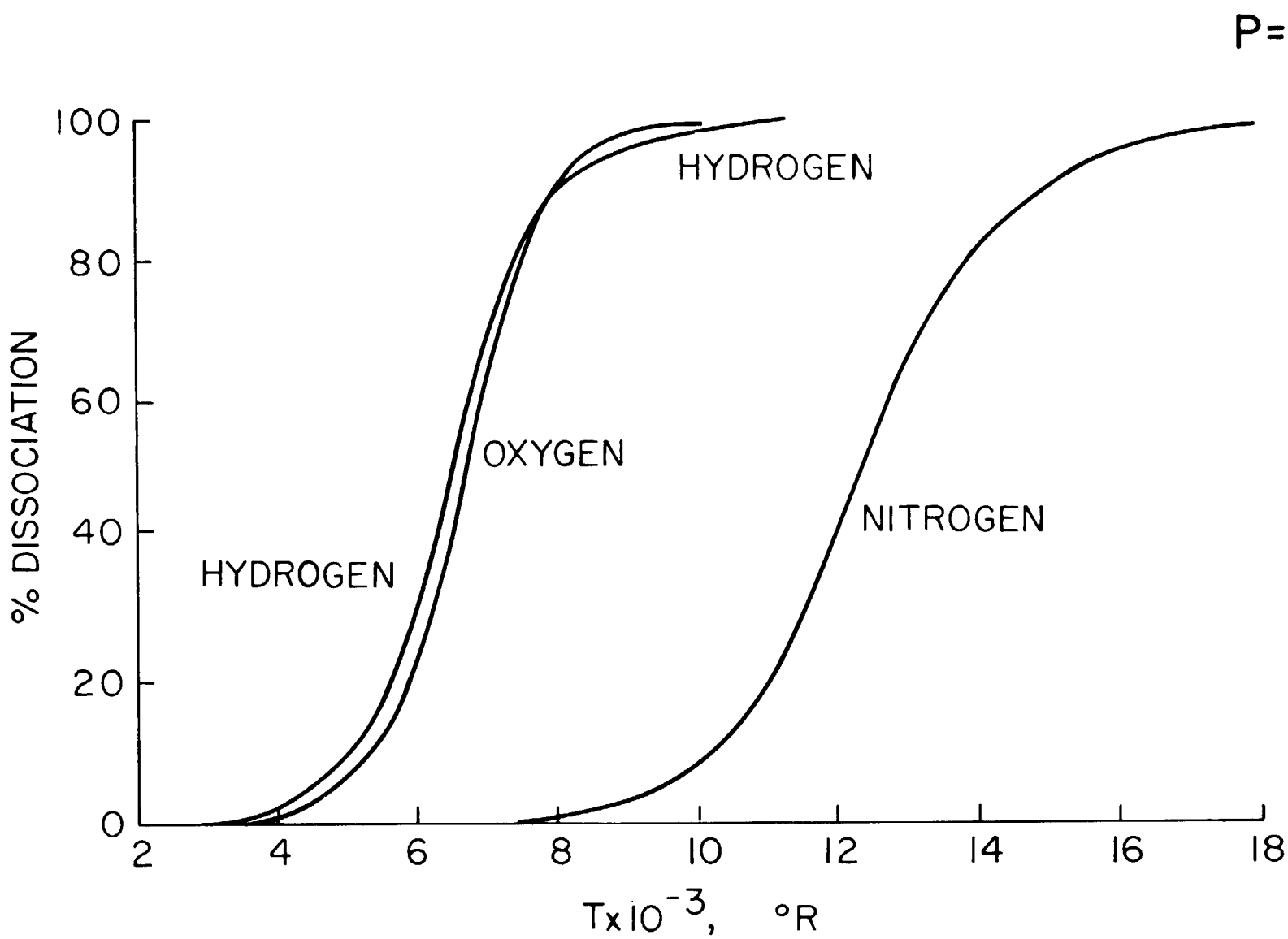

Figure 3. Equilibrium Dissociation of the Diatomic Gases

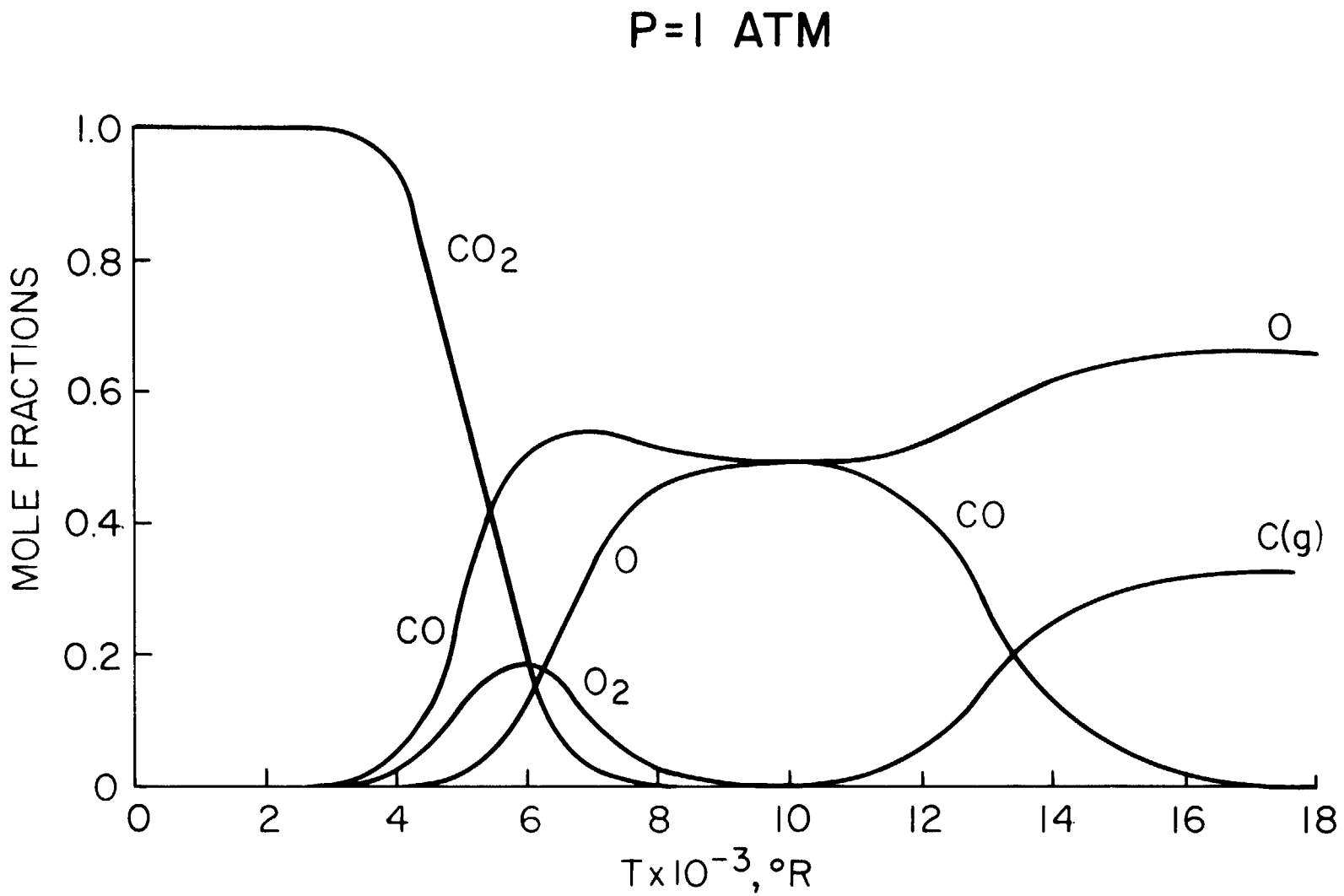

Figure 4. Equilibrium Dissociation of Carbon Dioxide

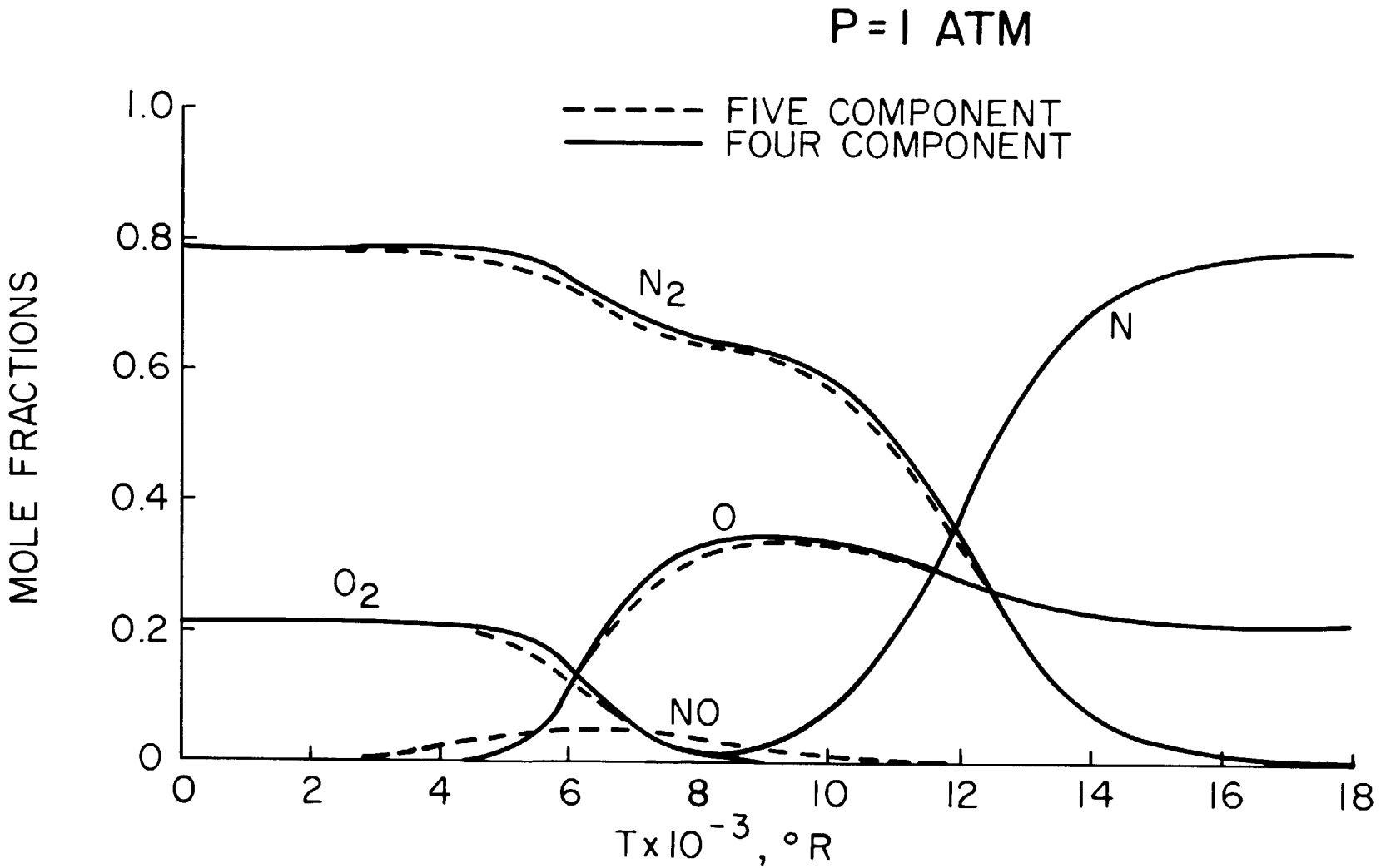

Figure 5. Equilibrium Dissociation of Four and Five Component Air

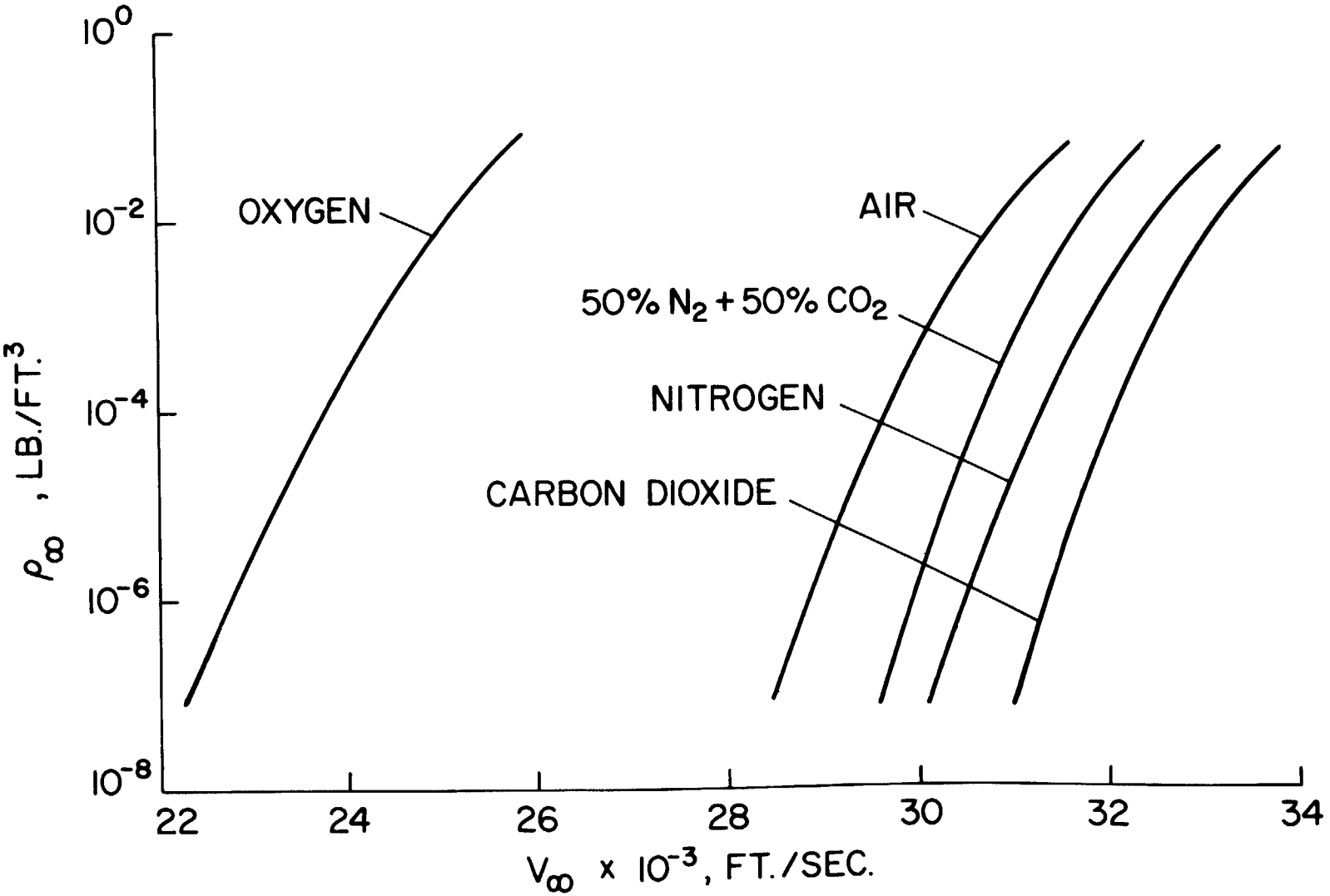

Figure 6. Ambient Densities and Flight Velocities at Approximately One Per Cent Ionization

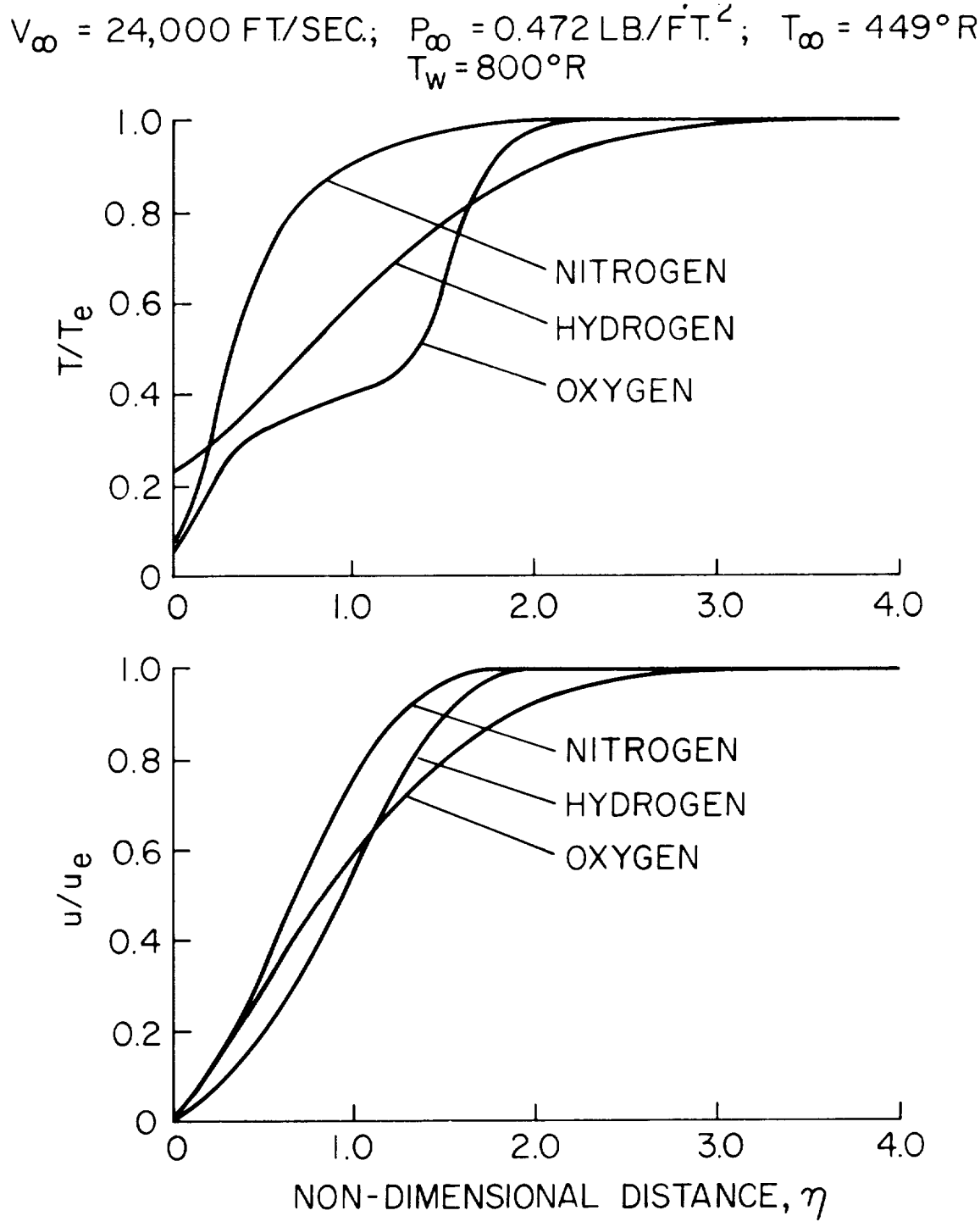

Figure 7. Temperature and Velocity Profiles (Diatomic Gases)

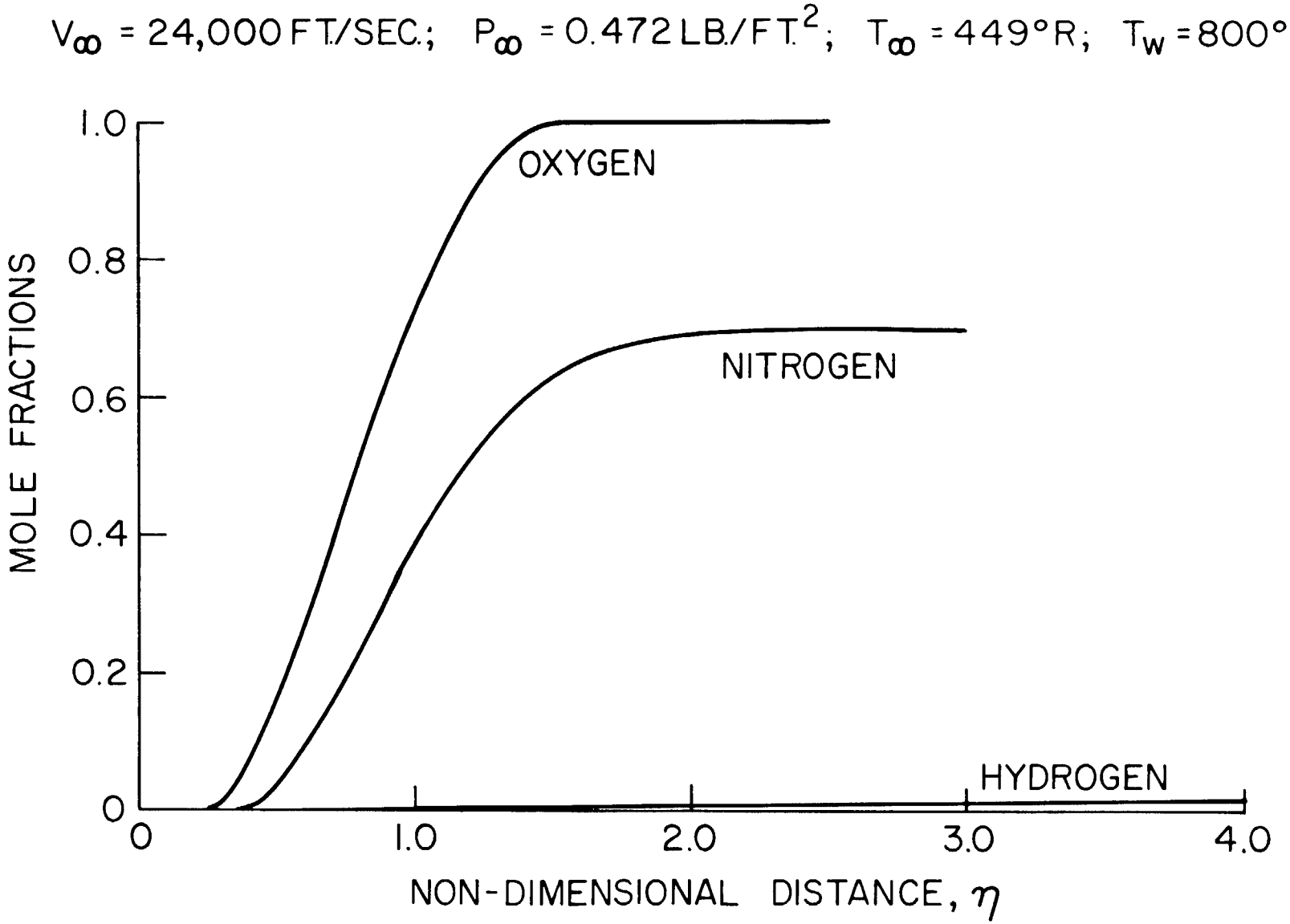

Figure 8. Variation of Atomic Species Through the Boundary Layer (Diatomic Gases)

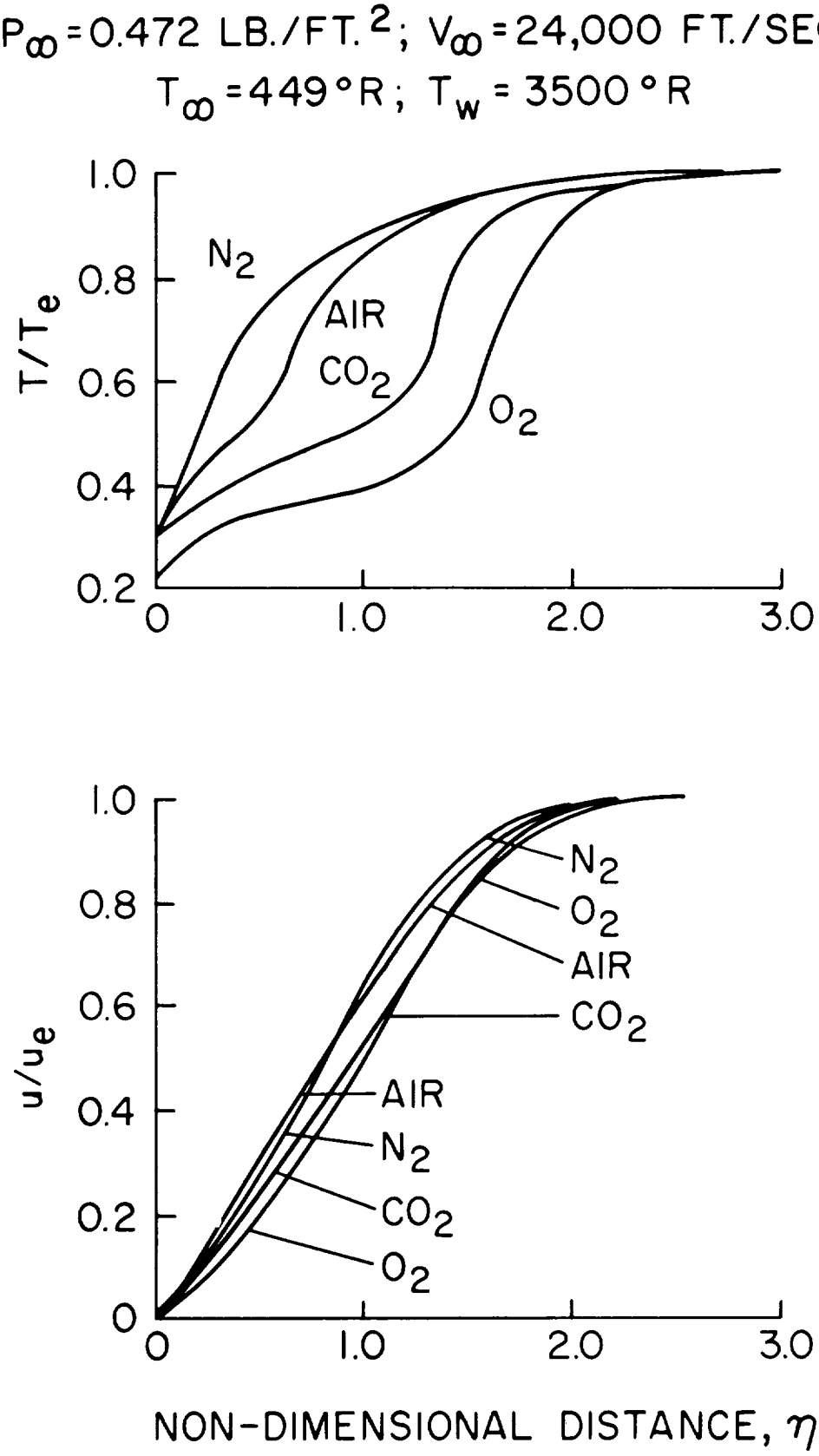

Figure 9. Temperature and Velocity Profiles (N_2, O_2, Air, CO_2)

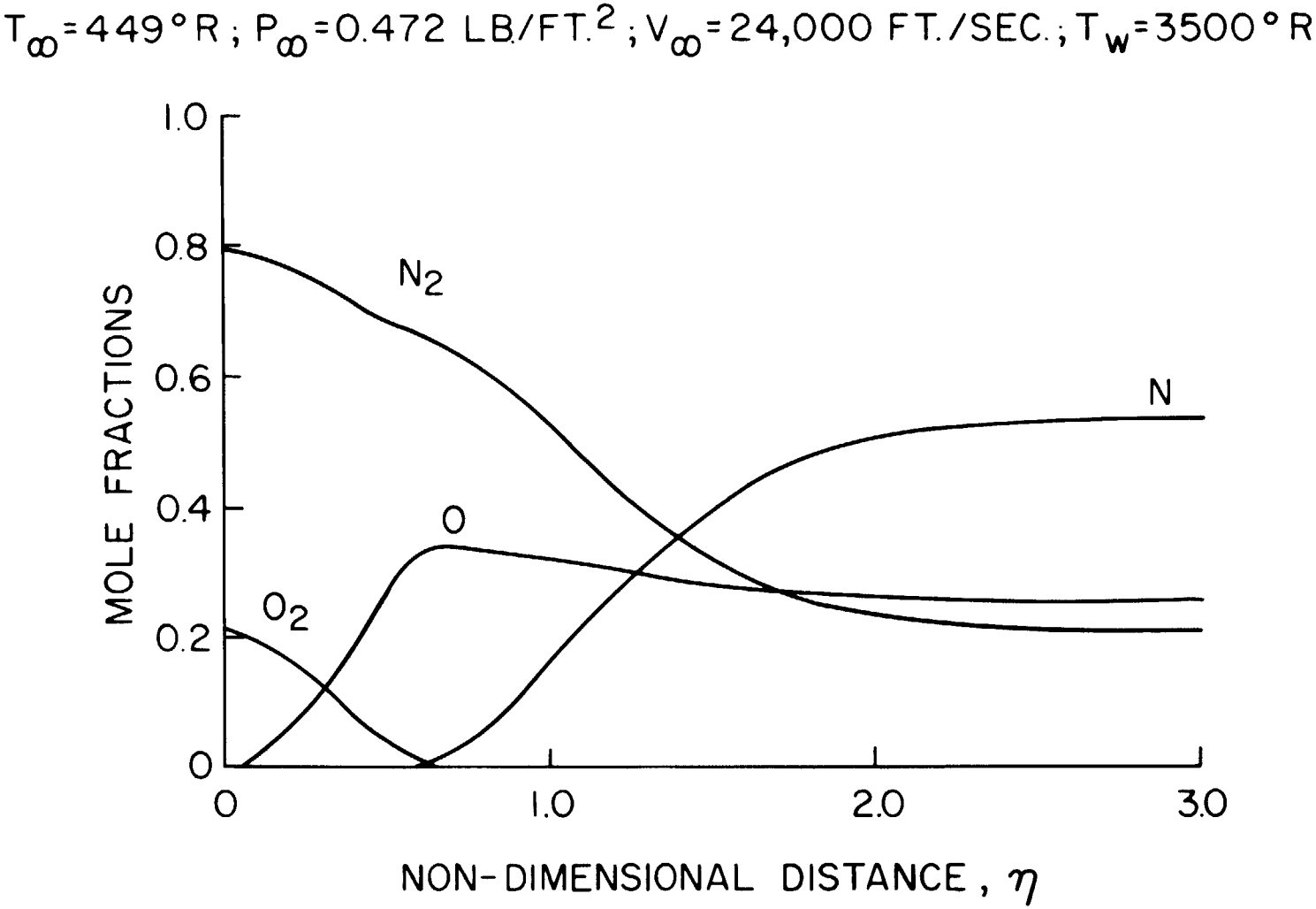

Figure 10. Boundary Layer Composition (Four Component Air)

$T_\infty = 449°R$; $P_\infty = 0.472$ LB./FT.^{2}; $V_\infty = 24{,}000$ FT./SEC.; $T_w = 3500°R$

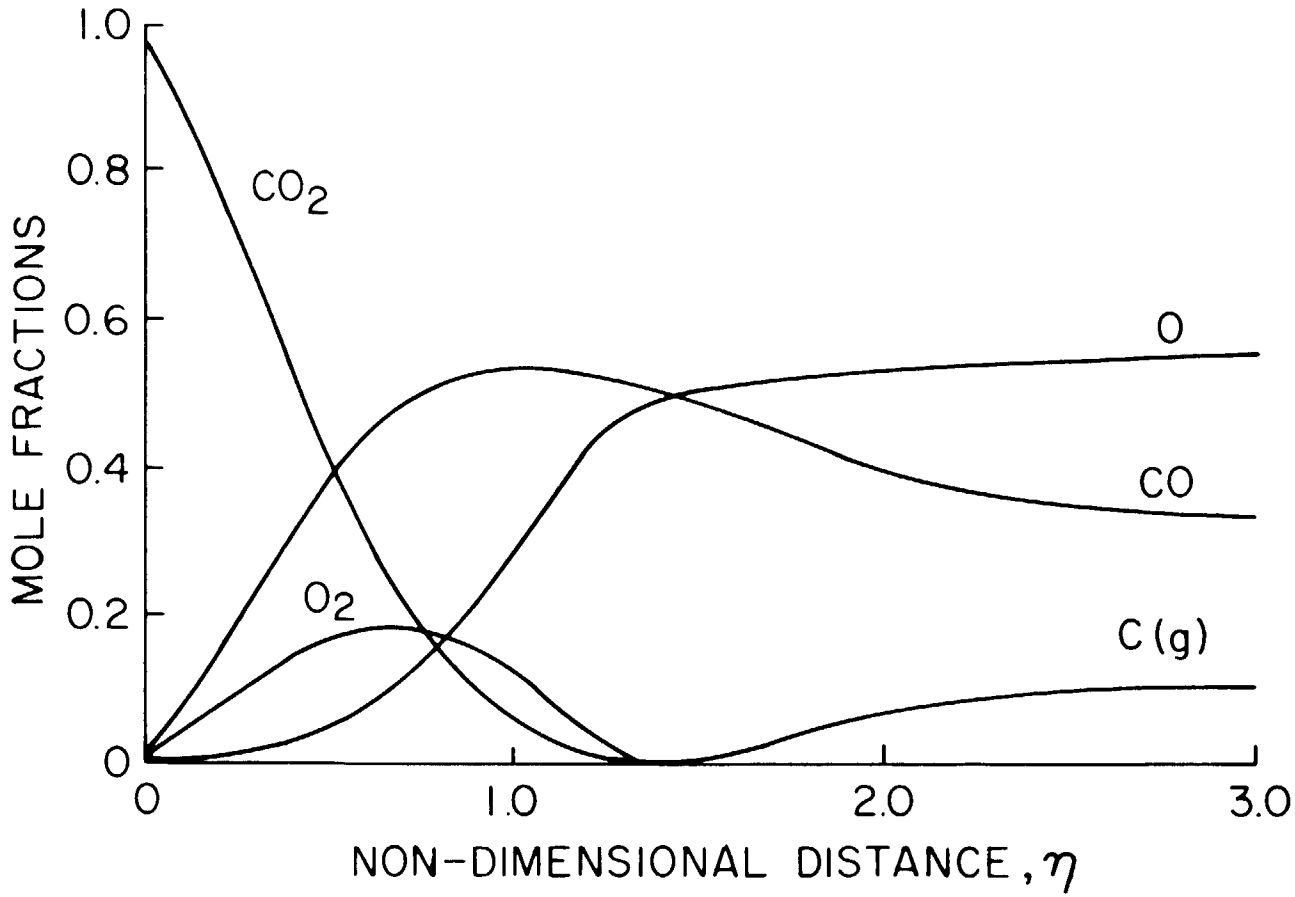

Figure 11. Boundary Layer Composition (Carbon Dioxide)

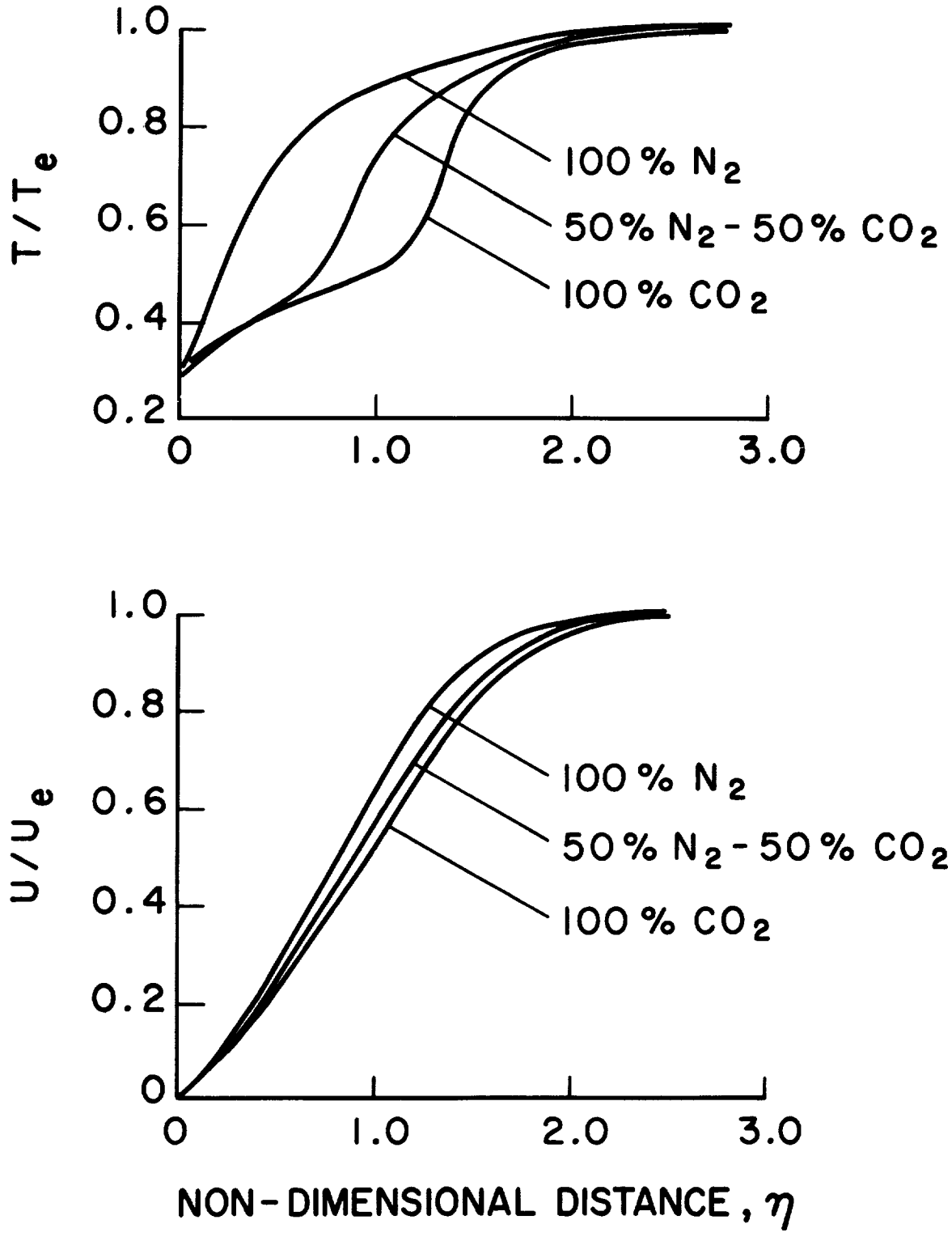

Figure 12. Temperature and Velocity Profiles
$T_\infty = 449^\circ R$, $P = 0.472\ lb/ft^2$
$V_\infty = 24,000\ ft/sec$, $T_W = 3500^\circ R$

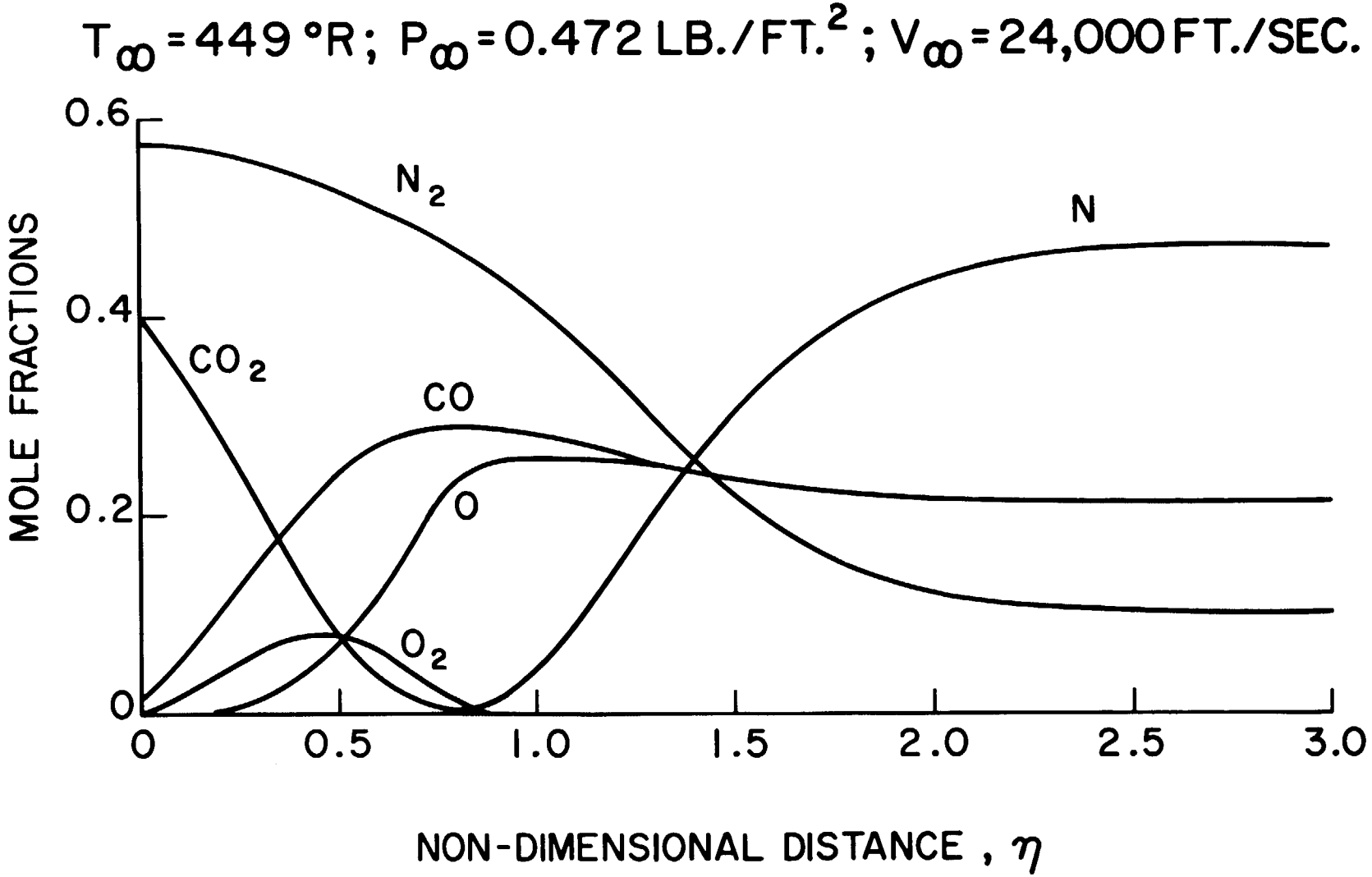

Figure 13. Boundary Layer Composition (50% N_2 -50% CO_2)

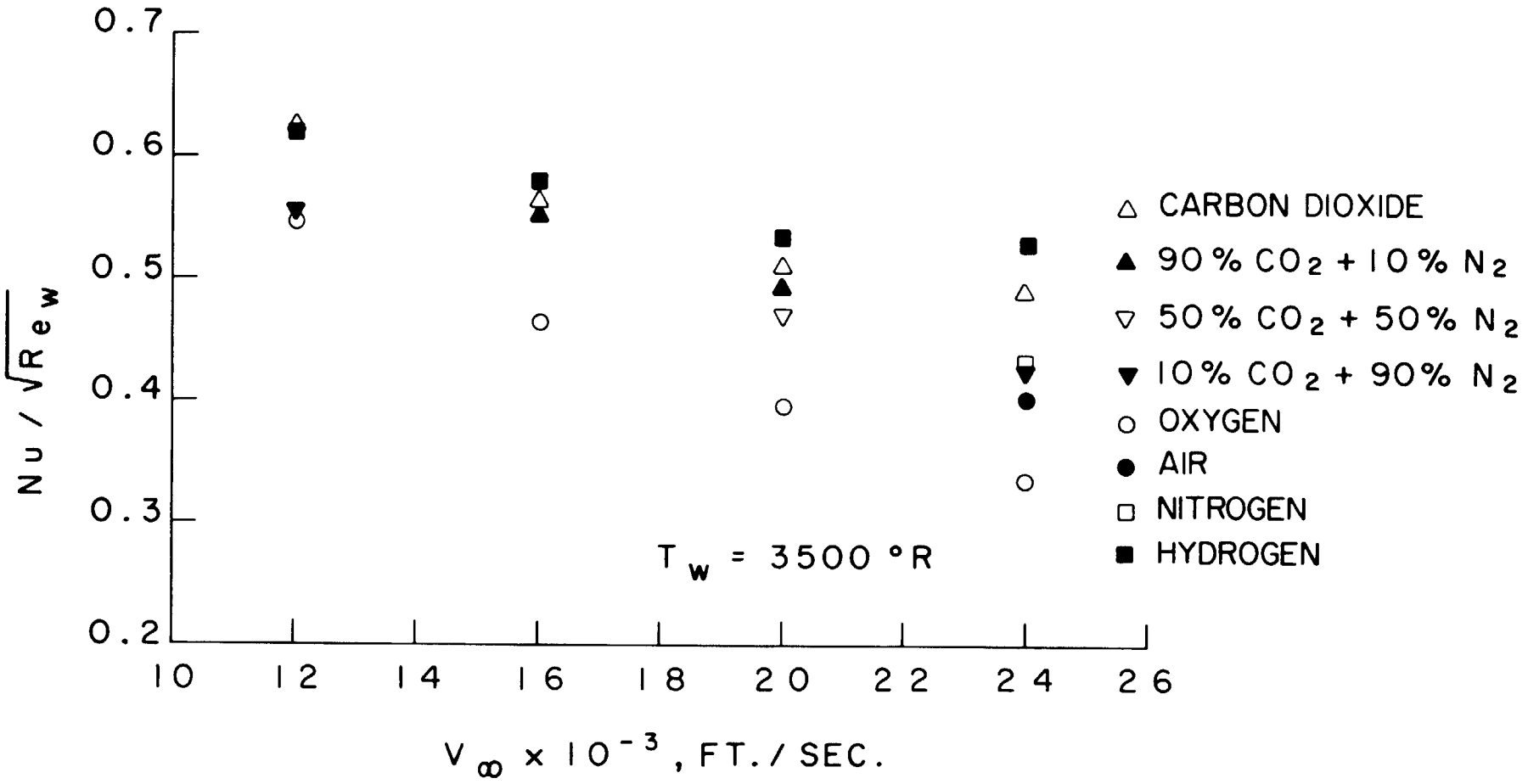

Figure 14. Variation of the Nusselt Number with Flight Speed

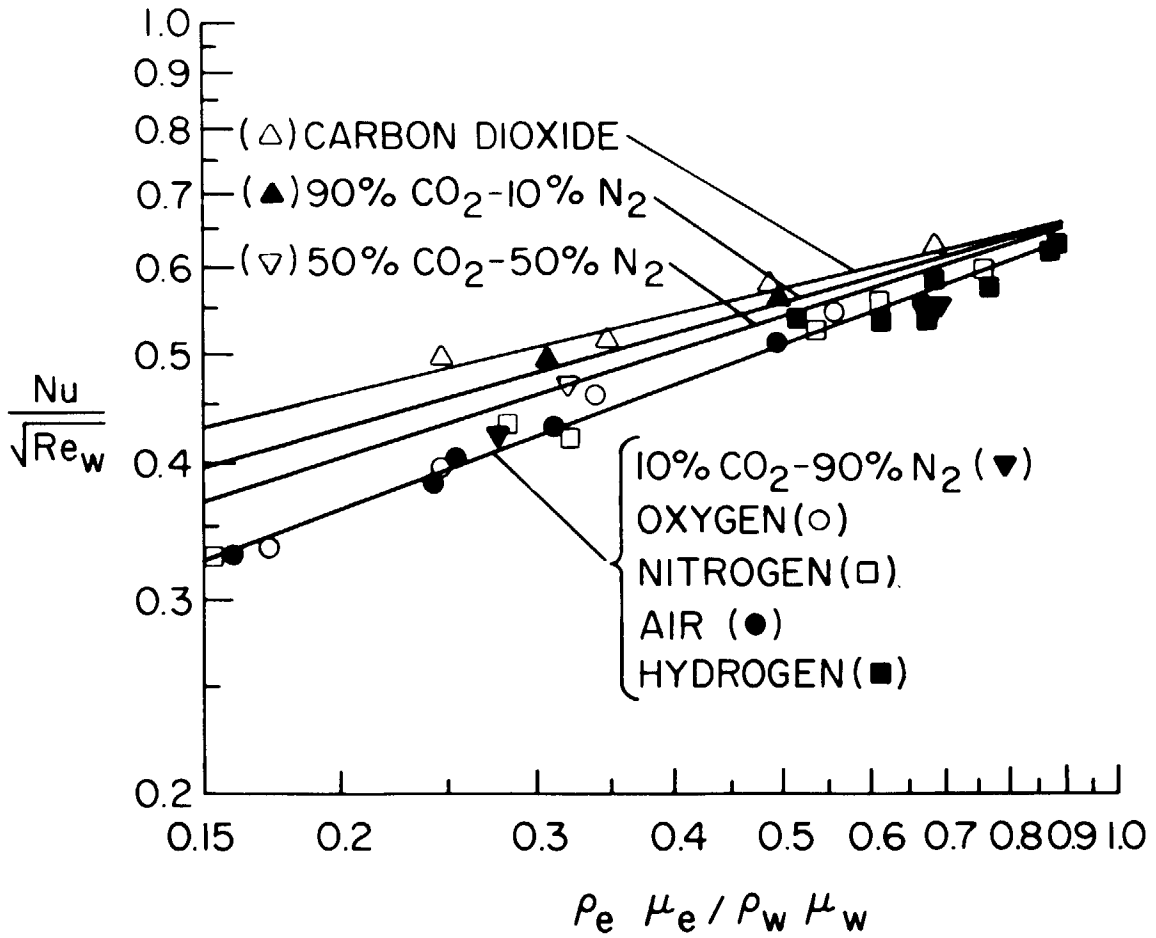

Figure 15. Variation of the Nusselt Number with Product of Density and Viscosity

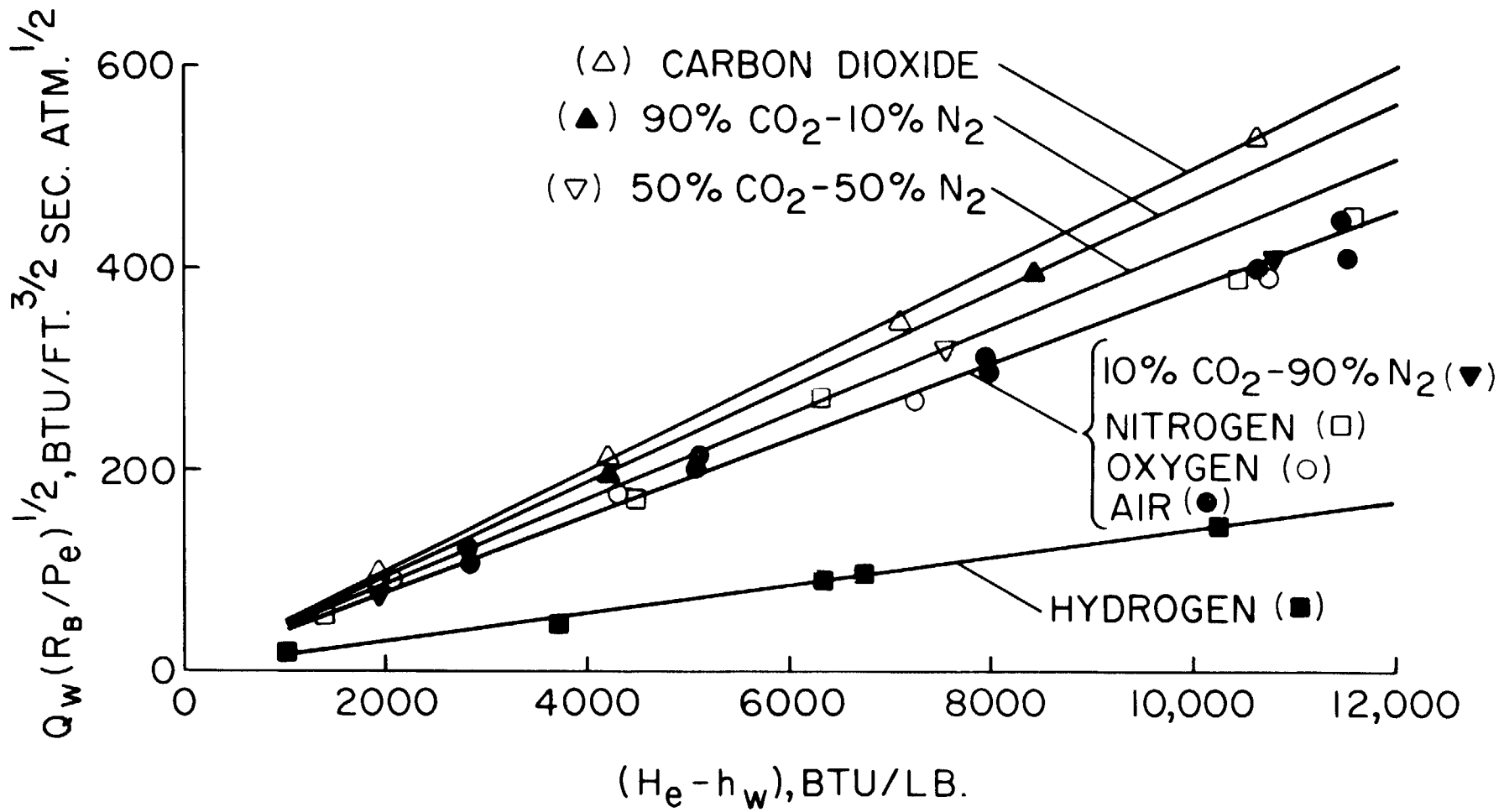

Figure 16. Variation of Correlated Heating Rates with Enthalpy Difference

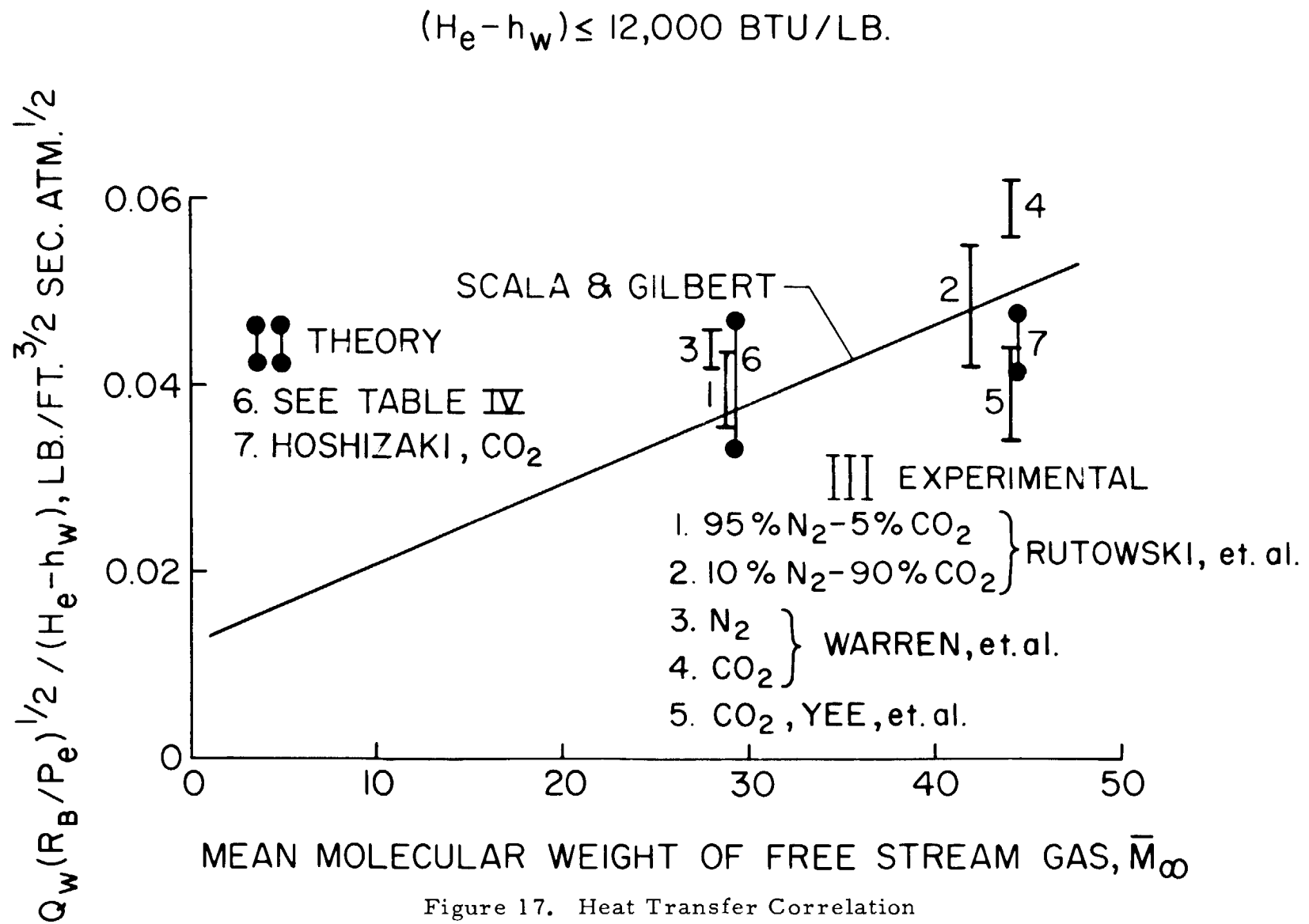

Figure 17. Heat Transfer Correlation

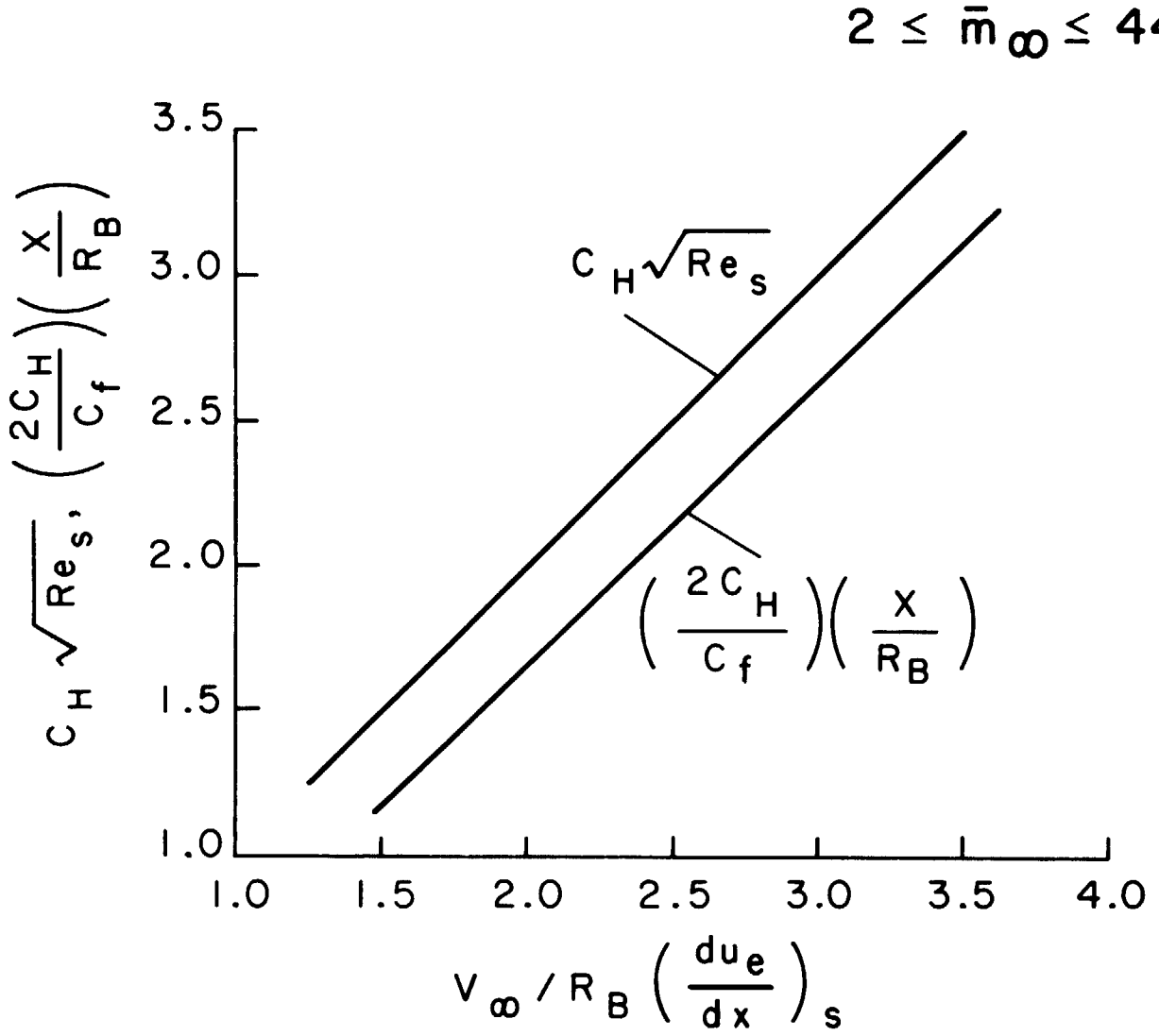

Figure 18. Correlation of the Stanton Number and Skin Friction Coefficients

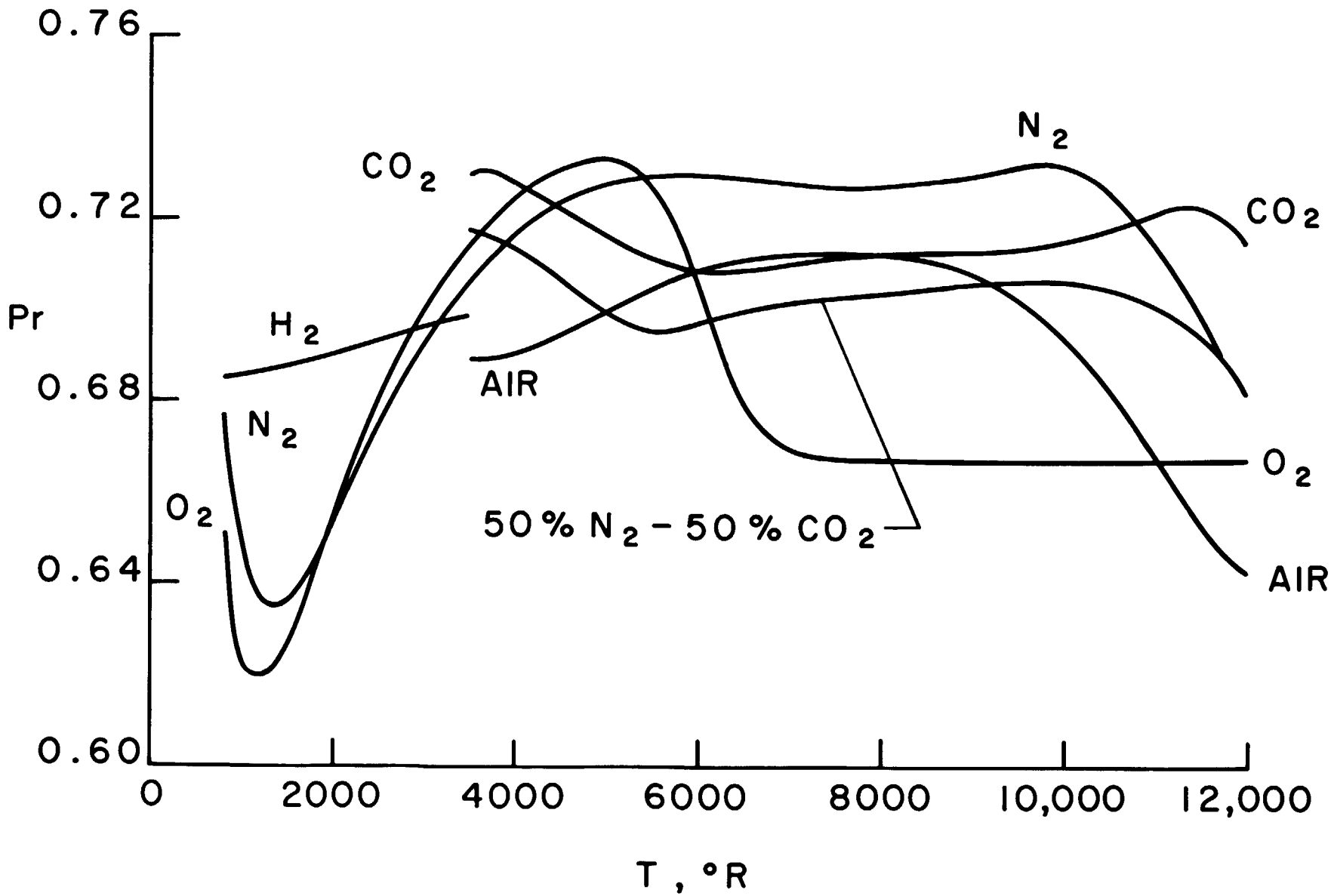

Figure 19. Prandtl Numbers for the Equilibrium Dissociated Mixtures

(P_∞ = 0.4715 lb/ft^2, T_∞ = 449°R, V_∞ = 24,000 ft/sec)

GENERAL ELECTRIC

SPACE SCIENCES LABORATORY
MISSILE AND SPACE DIVISION

TECHNICAL INFORMATION SERIES

AUTHOR	SUBJECT CLASSIFICATION	NO.
S. M. Scala L. M. Gilbert	Hypersonic Heat Transfer, Boundary Layer Theory	R63SD40
		DATE April, 1963
TITLE THEORY OF HYPERSONIC LAMINAR STAGNATION REGION HEAT TRANSFER IN DISSOCIATING GASES		G. E. CLASS I
		GOV. CLASS Unclassified
REPRODUCIBLE COPY FILED AT MSD LIBRARY, DOCUMENTS LIBRARY UNIT, VALLEY FORGE SPACE TECHNOLOGY CENTER, KING OF PRUSSIA, PA.		NO. PAGES 68

Abstract

This paper presents an investigation of the thermochemical effects of foreign planetary atmospheres upon hypersonic laminar stagnation region heat transfer and skin friction. Eight different dissociating gas mixtures were treated and the effects of molecular weight were correlated, over a range of free stream molecular weight between 2 and 44.

Conclusions

The most important single result obtained was that a correlation of all of the numerical results to a high order system of non-linear differential equations (i.e., the hypersonic boundary layer equations) yielded the following simple formula for hypersonic laminar stagnation region heat transfer in terms of the free stream molecular weight.

$$\frac{Q_w \sqrt{R_B}}{\sqrt{P_e}(H_e - h_w)} = (12.0 + 0.866\,\bar{m}_\infty) \times 10^{-3}$$

where Q_w is the heat transfer rate in Btu/ft^2 sec, P_e is the local pressure in atm, R_B in ft., and H_e and h_w are in BTU/lb.

By cutting out this rectangle and folding on the center line, the above information can be fitted into a standard card file.

AUTHOR S. M. Scala — Leon M. Gilbert
Sinclaire M. Scala — Leon M. Gilbert

COUNTERSIGNED Joseph Farber
Joseph Farber